2008

Nucleus Paragigantocellularis Afferents in Male and Female Rats: Organization, Gonadal Steroid Receptor Expression, and Activation During Sexual Behavior

Joseph J. Normandin

Anne Z. Murphy PhD
Georgia State University, amurphy@gsu.edu

Recommended Citation

Nomandin, J., & Murphy, A. Z. (2008). Nucleus paragigantocellularis afferents in male and female rats: Organization, gonadal steroid sensitivity, and activation during sexual behavior. *Journal of Comparative Neurology, 508*(5), 771-94. doi:10.1002/cne.21704

Nucleus Paragigantocellularis Afferents in Male and Female Rats: Organization, Gonadal Steroid Receptor Expression, and Activation During Sexual Behavior

Joseph J. Normandin and Anne Z. Murphy

Center for Behavioral Neuroscience, Department of Biology, Georgia State University, Atlanta, GA, 30303, USA

Running Head: nPGi afferents in male and female rats

Attention: Gert Holstege, Associate Editor

Key Words: sex, erection, ejaculation, Fos, estrogen, androgen

Corresponding Author: Anne Z. Murphy

Address: Georgia State University, Kell Hall 402, 24 Peachtree Center Avenue, Atlanta, GA, 30303, USA

Phone: 404-463-9661

Fax: 404-413-5301

E-mail: amurphy@gsu.edu

Supported by: National Institutes of Health; Grant DA16272 (to A.Z.M), and National Science Foundation; Grant IBN9876754 to the Center for Behavioral Neuroscience

Abstract

The supraspinal regulation of genital reflexes is poorly understood. The brainstem nucleus paragigantocellularis (nPGi) of rats is a well-established source of tonic inhibition of genital reflexes. However the organization, gonadal steroid receptor expression, and activity of nPGi afferents during sex have not been fully characterized in male and female rats. To delineate the anatomical and physiological organization of nPGi afferents, the retrograde tracer Fluorogold (FG) was injected into the nPGi of sexually experienced male and female rats. Animals engaged in sexual behavior one hour before sacrifice. Cells containing FG, estrogen receptor alpha (ER_α), androgen receptor (AR), and the immediate-early gene product Fos were identified immunocytochemically. Retrograde labeling from the nPGi was prominent in the bed nucleus of the stria terminalis, paraventricular nucleus (PVN) posterior hypothalamus, precommissural nucleus, deep mesencephalic nucleus, and periaqueductal gray (PAG) of both sexes. Sex differences were observed in the caudal medial preoptic area (MPO), with significantly more FG+ cells observed in males and in the PAG and inferior colliculus where significantly more FG+ cells were observed in females. The majority of regions that contained FG+ cells also contained ER_α or AR, indicating sensitivity to gonadal steroids. The proportions of FG+ cells that co-localized with sex-induced Fos was high in the PVN of both sexes, high in the MPO of males, but low in the PAG of both sexes despite the large number of PAG-nPGi output neurons and Fos+ cells in both sexes. The characterization of these afferents will lead to a further understanding of the neural regulation of genital reflexes.

Introduction

Genital reflexes in males and females subserve critical functions in reproductive biology. Despite this obvious importance, little is known about the supraspinal control of these reflexes. Dysfunctions within these systems contribute to, or are the basis of, sexual dysfunctions which produce profound disruptions not only in fertility, but also in quality of life experiences (Cameron and Tomlin, 2007; Laumann et al., 1999). Across the lifespan, approximately 31% percent of men will experience sexual dysfunction, including an inability to achieve an erection and/or premature or delayed ejaculation (Laumann et al., 1999). Similarly, 43% of women will experience some form of female sexual dysfunction, including involuntary vaginal spasms, painful sensations during penetration, and/or early or delayed orgasm (Laumann et al., 1999). Our understanding of the supraspinal control of genital reflexes is an important contribution to understanding and treating sexual disorders.

Studies in male rats have identified the nucleus paragigantocellularis (nPGi) of the brainstem as the primary source of tonic descending inhibition of erectile and ejaculatory reflexes. Projections from the nPGi terminate onto the spinal motor neurons that innervate the bulbospongiosus and ischiocavernosus muscles (Hermann et al., 2003; Murphy and Marson, 2000; Tang et al., 1999); these muscles are critical to the control of erection and ejaculation (Holmes et al., 1991; McKenna and Nadelhaft, 1986). Bilateral lesions of the nPGi in male rats decrease mount and intromission frequency, ejaculation latency, and increase the number of ejaculations to satiety (Yells et al., 1992; Yells et al., 1994). Lesions of the nPGi also decrease the latency, and increase the number of ex copula erections (Marson et al., 1992). By contrast, electrical stimulation of nPGi neurons results in an increased latency, and decreased amplitude of firing in motor neurons associated with genital reflexes (Johnson and Hubscher, 1998).

Interestingly, nPGi lesions do not alter the number of non-contact erections in males exposed to females behind a wire mesh screen (Liu and Sachs, 1999), suggesting that nPGi modulation of penile reflexes is context dependent. How this context is signaled to the nPGi remains to be elucidated.

The central regulation of the nPGi is poorly understood. In males rats, both the medial preoptic area (Murphy et al., 1999a) and the midbrain periaqueductal gray (Lovick, 1986; Murphy and Hoffman, 2001) send direct projections to the nPGi. Interestingly, MPO projections to the PAG terminate in close apposition to PAG projections to the nPGi, forming an indirect MPO-PAG-nPGi pathway in addition to the direct MPO-nPGi pathway (Murphy and Hoffman, 2001). In females, remarkably little is known regarding the anatomy and physiology of the nPGi. Spinally-projecting nPGi efferents terminate among the motor neurons involved in the urethrogenital reflex (Marson et al., 2003), and trans-synaptic retrograde tracer injection into rat clitoris (Marson, 1995), cervix (Lee and Erskine, 2000), and vagina/clitoris (Marson and Murphy, 2006) results in dense retrograde labeling in the nPGi. Similar to males, direct MPO projections to the nPGi of female rats have been reported (Marson and Foley, 2004) and nPGi cells retrogradely labeled from rat vagina/clitoris with a trans-neuronal tracer were associated with terminals from the MPO and PAG (Marson and Murphy, 2006). Contributions of other central sites of input to the nPGi in females remain to be described.

The nPGi can be conceptualized as the final common output from supra-spinal sites involved in sexual behavior to the spinal cord motor neurons controlling genital reflexes. An integration of appropriate external and internal signals related to sexual behavior must occur to determine when it is appropriate for genital reflexes to be produced. The nPGi may be one such area where an integration of signals occurs. This study was conducted to comprehensively

characterize nPGi afferents as to their source, expression of gonadal steroid receptors, and activation during sexual behavior in male and female rats. Possible sex-differences in the anatomical and/or physiological organization of this circuit were also examined.

Methods

Subjects

Adult male (n=56) and female (n=88) Sprague-Dawley rats (Zivic Laboratories Inc., Pittsburgh, PA) were used in these experiments. Animals were weight-matched (250-300 g) and housed in same-sex pairs in separate rooms on a 12:12 hour light:dark cycle (lights on at 7:00AM). Animals used in the sexual behavior studies were housed in reverse light cycle (lights off at 7:00AM). Access to food and water was ad libitum throughout the experiment, except during surgery. These studies were performed in strict compliance with the Institutional Animal Care and Use Committee at Georgia State University. All efforts were made to minimize any possible suffering by the animal, and to reduce the number of animals used.

Fluorogold Injections

Rats were anesthetized with ketamine/xylazine/acepromazine (50 mg/kg, 3.3 mg/kg, 3.3 mg/kg; i.p.; Henry Schein, Melville, NY) and placed in a stereotaxic frame upon achieving a deep surgical plane of anesthesia. The skull was adjusted so that Bregma and lambda were at the same dorsoventral plane. Glass micropipettes (10-20 μm) were filled with the retrograde tracer Fluorogold (FG; 2% soln. w/v in saline; Fluorochrome LLC, Denver, CO) and lowered into the nPGi at the following coordinates (in mm): AP: -2.0 Lambda; ML: -1.0; DV: -8.5. FG was iontophoresed (50% duty cycle, 7.5 μA current) for 20 min. Pipettes remained in place for five minutes after injection to prevent backflow of tracer along the pipette tract and to facilitate

neuronal uptake. Special care was taken to ensure that all injection protocols were comparable for males and females. Following surgery the animals were allowed to recover under a heat lamp in clean cages, and returned to their original housing facilities upon recovery from the anesthetic. Animals were sacrificed 10 days after FG injections.

Sexual Behavior

A subset of our FG injected intact males (n=44) and females (n=36) rats engaged in three one hour mating bouts with stimulus animals before injection of FG. All females were ovariectomized and hormone-primed (10 µg estradiol in sesame oil 48 hours before mating, 500 µg progesterone in sesame oil) 4 hours before mating. Mating took place in a 60 cm x 30 cm transparent acrylic arena. Experimental males had free access to stimulus females, whereas experimental females engaged in paced-mating with a separator in the arena (with two 4 cm diameter holes through which only females could fit). Following retrograde tracer injections, the rats engaged in three additional one hour mating bouts, and were sacrificed on the last mating bout one hour after producing or receiving (male and females respectively) an ejaculation.

Perfusion fixation

Animals were given a euthanizing dose of sodium pentobarbital (160 mg/kg, i.p.; Sigma-Aldrich, St. Louis, MO) and perfused transcardially with 100-200 ml of 0.9% sodium chloride containing 2% sodium nitrite as a vasodilator, followed immediately by 250 ml of 4% paraformaldehyde in 0.1M phosphate buffer containing 2.5% acrolein (Polysciences Inc., Warrington, PA). Following fixation, a final rinse (100-200 ml) with the sodium chloride/sodium nitrate solution was used to remove any residual acrolein from the animal. Immediately following perfusion, the brains were removed and stored at 4°C in 30% sucrose solution until sectioned. The brains were cut into 25 µm coronal sections with a Leica 2000R freezing

microtome and stored free-floating in cryoprotectant-antifreeze solution (Watson et al., 1986) at –20°C until immunocytochemical processing was initiated.

Immunocytochemistry

A 1:6 series through the rostrocaudal axis of each brain was processed for FG and estrogen receptor alpha (ER_α), FG and androgen receptor (AR), or FG and the immediate-early gene product Fos as previously described (Loyd and Murphy, 2006; Murphy and Hoffman, 2001). Briefly, sections were removed from the cryoprotectant-antifreeze solution, rinsed extensively in potassium phosphate-buffered saline (pH 7.4), and then reacted for 20 minutes in 1% sodium borohydride to remove excess aldehydes. Sections were then incubated in primary antibody solution directed against either ER_α, AR, or Fos in potassium phosphate buffered saline (KPBS) containing 0.1% Triton-X for 1 hour at room temperature followed by 48 hours at 4°C. Cells containing ER_α were identified using a polyclonal rabbit anti-ER_α antibody (Santa Cruz Biotech Inc., sc-542, Lot: B1505, Santa Cruz, CA) at a concentration of 1:20,000. This rabbit antiserum was prepared against a peptide mapping at the C-terminus of ER_α of mouse origin (HSLQTYYIPPEAEGFPNTI) corresponding to amino acids 580-599 (manufacturer's technical information), and specificity of this antibody has been confirmed by preabsorbtion with epitope peptide (Quesada et al., 2007). Cells containing AR were identified using the polyclonal rabbit anti-AR antibody (Santa Cruz Biotech Inc., sc-816, Lot: B0204, Santa Cruz, CA) at a concentration of 1:10,000. This rabbit antiserum was prepared against a peptide mapping at the N-terminus of AR of human origin (MEVQLGLGRVYPRPPSKTYRG) corresponding to amino acids 2-21 (manufacturer's technical information), and specificity of this antibody has been confirmed by preabsorbtion with epitope peptide (Creutz and Kritzer, 2004). Cells containing Fos were identified using the polyclonal rabbit anti-Fos antibody (Calbiochem, PC38, Lot: 4191,

San Diego, CA) at a concentration of 1:700,000. This rabbit antiserum was prepared against a synthetic peptide (SGFNADYEASSSRC) corresponding to amino acids 4-17 of human c-Fos, and specificity of this antibody has been confirmed by preabsorbtion with epitope peptide (Sun et al., 2007). In Western blots, this antibody recognizes the ~55 kDa c-Fos and ~62 kDa c-Fos proteins, and does not cross-react with the ~39 kDa Jun protein (manufacturer's technical information).

After primary antibody incubation, the tissue was rinsed in KPBS, incubated for 1 hour in biotinylated goat anti-rabbit IgG (Jackson Immunoresearch Labs Inc., West Grove, PA) at a concentration of 1:600, rinsed in KPBS, followed by a 1 hour incubation in avidin-biotin peroxidase complex (Vector Labs, ABC Elite Kit PK-6100, Burlingame, CA) at a concentration of 1:10. After rinsing in KPBS and sodium acetate (0.175 M; pH 6.5), ER_{α}, AR, and Fos were visualized as a black reaction product using nickel sulfate intensified 3,3'-diaminobenzidine solution containing 0.08% hydrogen peroxide in sodium acetate buffer. The reaction product was terminated after approximately 30 minutes by rinsing in sodium acetate buffer. Tissue was then processed for FG immunoreactivity as above. Cells containing FG were identified using the polyclonal rabbit anti-Fluorogold antibody (Chemicon, AB153, Lot: 25060005, Temecula, CA) at a concentration of 1:30,000. This antibody was raised against the chemical compound hydroxystildamidine (Fluorogold; manufacturer's technical information). No cytoplasmic FG+ staining was present in animals in which the tracer failed to be ejected from the electrode. FG was visualized as a brown reaction product using 3,3'-diaminobenzidine containing 0.08% hydrogen peroxide in Tris buffer (pH 7.2). The reaction product was terminated after approximately 30 minutes by rinsing in Tris buffer. Sections were mounted out of saline onto

gelatin-subbed slides, air dried overnight, dehydrated in a series of graded alcohols, cleared in Histoclear, and cover-slipped using Histomount.

Data Analysis and Presentation

A single individual conducted all analyses. Animals were coded to blind the counter to sex and animal number. Injection sites were subjectively graded with respect to their location and spread. Only those animals with injections that corresponded to a focal point within the nPGi were selected for cell counting (see Figure 1). Thirteen males and 15 females had injections that met our strict and conservative criteria. Of these animals, all were used for our retrograde tracing analysis, 6 males and 7 females were used in our retrograde tracer/gonadal-steroid receptor expression analysis, and 5 males and 6 females were used in our retrograde tracer/sexual behavior-induced Fos expression analysis.

Missed injections dorsal or lateral to the nPGi (i.e. into the pyramidal tract) were examined for specificity of retrograde tracing in target injections. All regions containing FG labeling were examined. The MPO and PAG were additionally subdivided into four (Bregma -0.26, -0.30, -0.40, -0.80) and six (Bregma -5.30, -6.04, -6.80, -7.64, -8.30, -8.80) rostrocaudal levels, respectively. Counts for FG+, ER_{α}/FG+, AR/FG+, or Fos/FG+ cells were determined on the side ipsilateral to the injection site, and FG+ labeling on the side contralateral to the injection site were noted, but not counted. FG+ cells were easily identifiable based on the brown reaction product in the cytoplasm. FG+ cells that contained ER_{α}, AR, or Fos were readily identifiable based on the black reaction product restricted to the nucleus. The minimum distance between any two sections analyzed was 40 µm (Bregma -0.26 and -0.30). The majority of retrograde labeling in this area was observed in the MPO, where the maximum diameter of the largest cells can be expected to be approximately 12 µm (calculated from (Madeira et al., 1999); therefore

cell counts between these sections (and any two sections) are independent and do not reflect duplicate counting of cells.

Single and dual-labeled cells were plotted and quantified across the rostrocaudal axis of the rat brain based on the atlas of (Paxinos and Watson, 1997). The mean and standard error of the mean (SEM) of FG+, ER_α/FG+, AR/FG+, and Fos/FG+ cells for each sex, section, and region of interest were calculated. We use the term "density" within this manuscript as shorthand for the number or proportion of cells observed within a given brain region. The relative density of FG+ labeled cells was defined as sparse when <25 labeled cells were observed and dense when ≥25 cells were observed. The relative density of the percent co-localization of FG+ cells with ER_α, AR, or Fos was defined as low when <10%, moderate when between 10% and 24%, and high when >25%.

Behavioral measures for our sexual behavior-induced Fos experiments include the average number of mounts (M), intromissions (I), and ejaculations (E) in males, and the average number of M/I/E received, lordosis quotient (LQ; lordosis/M+I+E received), and lordosis rating (LR; magnitude of dorsoflexion; 0 = none, 1 = slight, 2 = full) as defined in (Pfaus, 1996).

Statistical comparisons of FG+, ER_α/FG+, AR/FG+, and Fos/FG+ cell numbers were made between males and females for regions providing dense input to the nPGi. T-tests were used for mean comparisons and differences were considered significant at the alpha ≤0.05 level for planned comparisons of the MPO and PAG. The family-wise alpha level (≤0.05) was adjusted to ≤0.0031 using the Bonferroni method for the sixteen unplanned comparisons.

For data presentation, a representative animal from each experimental group was selected and the distribution of FG+, ER_α/FG+, AR/FG+, and Fos/FG+ cells were plotted using a Nikon Drawing Tube attached to a Nikon Optiphot microscope. Plots were scanned, imported to a

computer, and finalized using Adobe Illustrator 10. Photomicrographs were generated using a Synsys digital camera attached to a Nikon Eclipse E800 microscope. Images were captured with QCapture and finalized using Adobe Photoshop 7.0. Alterations to the images were strictly limited to enhancement of brightness/contrast.

Results

Injections Sites

Injections were centered within the rostral portion of the nPGi with moderate spread to the pyramidal tract. Subjective blind ratings of injection quality did not differ between the sexes. Figure 1 shows a representative FG injection site within the nPGi of a male and female rat.

General Patterns in Labeling

Table 1 lists all regions that contained FG+ cells in male and female rats, weighted by density of FG+ cells and co-localization with ER_{α}, AR, or Fos. Regions ipsilateral to the injection site showed a qualitatively higher degree of retrograde labeling than contralateral regions. There were a few notable exceptions: the rostral parvicellular red nucleus (RPC) and rostral portion of the ventral nucleus of the lateral lemniscus in males, and the caudal portion of the RPC and the paralemniscal nucleus (PL) in females had a qualitatively higher degree of retrograde labeling on the side contralateral to the injection site.

Organization and Gonadal Steroid Receptor Expression of nPGi Afferents

Diencephalon. Representative plots of FG+, ER_{α}/FG+, and AR/FG+ cells in the diencephalic regions are shown in Figure 2. In both males and females, sparse FG labeling was observed in

the rostral MPO (Figure 2A-B). However, within the caudal half of MPO (Figure 2C-D), the number of FG+ cells increased significantly in males [p=0.014; Figure 3A]. FG labeling in the caudal MPO in males formed a discrete cell group that was not consistently observed in females (Figure 2D). The proportion of FG+ cells that contained ER_α varied for males and females along the rostrocaudal axis of MPO (Figure 3B). In the rostral pole of MPO, 33% of FG+ cells in females also contained ER_α, whereas only 9% of FG+ cells contained ER_α in males (Figure 3B). For the androgen receptor, at most rostrocaudal levels, males generally had a higher percent co-localization than females (average 37% AR/FG+ cells versus 18% in females), and males differed from females significantly at two rostrocaudal levels [Bregma -0.26, p=0.024 and Bregma -0.40, p=0.037; Figure 3C]. The lateral preoptic area was sparsely labeled for FG in both sexes.

In the bed nucleus of the stria terminalis (BNST; Figure 2A-D), retrograde labeling was primarily restricted to the caudal regions (Figure 2C-D) in both males and females (Figure 4A). ER_α and AR co-localization with FG+ caudal BNST cells was comparable in both sexes (approximately 30%; Figure 4B). With respect to the androgen receptor, 43% of FG+ caudal BNST cells contained AR in males, and 26% co-localized in females (Figure 4C).

Within the amygdala (Figure 2E-F), the medial amygdala exhibited sparse FG+ labeling in both sexes. In contrast, dense FG+ labeling was present in the central amygdala (CeM) in males, with less labeling observed in females (Figure 4A). ER_α co-localization with FG+ CeM cells was low in males (9%), and moderate in females (17%; Figure 4B). For AR, higher levels of co-localization in the CeM was observed in both sexes (between 40-50%; Figure 4C).

Dense FG+ labeling in the hypothalamus (Figure 2E-F) was observed in the paraventricular nucleus (PVN) and posterior hypothalamus (PH) of both sexes, and the

perifornical nucleus (PeF) in females (Figure 4A). Figure 5 shows an example of FG labeled cells in the PVN for males and females. These regions exhibited low levels of ER_{α} (Figure 4B) or AR (Figure 4C and 5) co-localization, with the exception of the PeF in males where 23% of FG+ cells contained AR (Figure 4C). Sparse FG+ labeling was present in the anterior hypothalamus, lateral hypothalamus, retrochiasmatic area, dorsomedial hypothalamus, ventromedial hypothalamus, arcuate nucleus, tuber cinereum area, and the magnocellular nucleus of the lateral hypothalamus in both sexes.

In the thalamus (Figure 2E-G) dense FG+ labeling was observed in the precommissural nucleus (PrC) in both sexes and the parafascicular thalamic nucleus (PF) in females (Figure 4A). ER_{α} co-localization with FG+ PrC cells was moderate in males (10%) and low in females (3%; Figure 4B). By contrast, AR co-localization with FG+ PrC cells was higher (males, 38%; females, 11%; Figure 4C). In the PF, while ER_{α} was present, there were no ER_{α}/FG+ cells observed. However, AR/FG+ cells were observed in males (28%) and females (12%; Figure 4C) in this same region. Sparse FG+ labeling was observed in the rostral interstitial nucleus of the medial longitudinal fasciculus, prerubral field, parvicellular subparafascicular nucleus, subincertal nucleus, and zona incerta in both sexes.

Mesencephalon. Representative plots of FG+, ER_{α}/FG+, and AR/FG+ labeling in the mesencephalic regions are shown in Figure 2. In the midbrain (Figure 2G-M), dense FG+ labeling was observed in the deep mesencephalic nucleus (DpMe) and intercollicular nucleus (InCo) in both sexes (Figure 4A), with low to moderate levels of ER_{α} co-localization (Figure 4B). A greater percentage of AR/FG+ cells were observed in males within the DpMe (23% versus 5% in females (Figure 4C). Sparse FG+ labeling was observed in the oculomotor

nucleus, Edinger-Wetsphal nucleus, nucleus of the posterior commissure, magnocellular nucleus of the posterior commissure, interstitial nucleus of the medial longitudinal fasciculus, RPC, retrorubral field, posterior intralaminar thalamic nucleus, peripeduncular nucleus, lateral substantia nigra, reticular substantia nigra, parabrachial pigmented nucleus, dorsal substantia nigra compacta, nucleus of the optic tract, posterior limitans thalamic nucleus, subbrachial nucleus, and the ventral tegmental area (VTA).

In both sexes, dense FG+ labeling was observed throughout the rostrocaudal axis of the PAG (Figure 2H-M). In the dorsomedial region (dmPAG), females consistently had a greater number of FG+ cells at all rostrocaudal levels [Bregma -5.30, p=0.009, Bregma -6.80, p=0.009, Bregma -7.64, p=0.001 and Bregma -8.30, p=0.029; Figure 6A]. Similar sex differences (females > males) were observed in the lateral [lPAG; Bregma -8.30, p=0.022] and ventrolateral regions of the PAG (Figure 6A). For the dmPAG and lPAG, the percentage of FG+ cells that also contained ER_{α} increased moving caudally through the PAG in both males and females. Interestingly, while females had a greater number of FG+ cells throughout the rostrocaudal axis of PAG, co-localization with ER_{α} or AR was generally higher in males (Figure 6B and 6C). Sparse FG+ labeling was observed in the dorsolateral PAG.

In the superior colliculus (Figure 2H-K) dense FG+ labeling was observed in the deep gray layer (DpG) in both sexes, and the rostral superior colliculus (rSC) in females (Figure 4A). Females had a greater number of FG+ cells in both the DpG and rSC. Little ER_{α} expression is present within the superior colliculus, and consequently steroid receptor co-localization with superior collicular FG+ cells was low or absent (Figure 4B). Despite the low amount of AR present in this region, AR/FG+ co-localization was higher in males than females in the DpG and

rSC (Figure 4C). Sparse FG+ labeling was observed in the optic nerve layer of the superior colliculus and intermediate gray layer of the superior colliculus.

Dense FG+ labeling was present in the inferior colliculus (Figure 2H-M) of both sexes. In the external cortex of the inferior colliculus (ECIC) the number of FG+ cells was significantly greater in females [p=0.002; Figure 4A]. Little ER_{α} and AR expression is present within the inferior colliculus in either sex, and consequently low levels ER_{α} or AR co-localization with FG+ cells in the ECIC were observed in both sexes (Figures 4B and 4C). Sparse labeling was observed in the brachium of the inferior colliculus in both sexes.

Metencephalon. Representative plots of FG+, ER_{α}/FG+, and AR/FG+ labeling in the metencephalic regions are shown in Figure 2. Dense pontine (Figure 2K-M) FG+ labeling was observed in the region of the motor root of the trigeminal nerve, possibly encompassing a caudal portion of the PL, in both sexes (Figure 4A). Little ER_{α} and AR expression is present within the pons, and consequently steroid receptor co-localization with pontine FG+ cells was low or absent (Figures 4B and 4C). Sparse FG+ labeling was observed in the retrorubral nucleus, pedunculopontine tegmental nucleus, cuneiform nucleus, dorsal tegmental bundle, parabrachial nucleus, laterodorsal tegmental nucleus, oral pontine reticular nucleus, motor trigeminal nucleus, ventrolateral tegmental area, and the olivary nuclei.

Myelencephalon. Representative plots of FG+, ER_{α}/FG+, and AR/FG+ labeling in the myelencephalic regions are shown in Figure 2. Dense medullary (Figure 2N-O) FG+ labeling was observed in the lateral reticular nucleus in both sexes and interpolar spinal trigeminal nucleus in females (Figure 4A). Little ER_{α} and AR expression is present within the

myelencephalon and consequently steroid receptor co-localization with medullary FG+ cells was absent (Figure 4B and 4C). Sparse FG+ labeling was observed in the locus coeruleus, nucleus of the solitary tract, cuneate nucleus, intermediate reticular nucleus, and the parvicellular reticular nucleus.

Activation of nPGi Afferents During Sexual Behavior

Several sexual behavior measures were quantified for the last mating bout (Table 2). These values are consistent with previous studies examining male and female sexual behavior (Pfaus, 1996).

Diencephalon. Representative plots of Fos/FG+ labeling in the diencephalic regions are shown in Figure 7. In the preoptic area (Figure 7A-D), the proportion of sex-induced Fos present in FG+ cells in males and females differed along the rostrocaudal axis. In the rostral MPO, females had a higher percentage of co-localization than males (24% versus 13%, respectively; Fig 8). By contrast, in the caudal MPO males had a higher percentage of Fos/FG+ cells than females (Figure 8). At mid levels of the MPO, 43% of FG+ cells contained Fos in males, in comparison to 20% in females [p=0.035]. Significant differences were also noted in the caudal MPO (32% Fos/FG+ cells in males, versus 15% in females [p=0.042]). In males, FG+ cells that co-localized with Fos formed a discrete group of cells that was rarely observed in females.

In the BNST (Figure 7A-D), while high levels of Fos was observed in both males and females, very few were present in FG+ cells (Figure 9). Similarly, in the CeM (Figure 7E-F), while moderate amounts of Fos were present in males and females, low levels of co-localization were observed in both sexes (Figure 9).

In the hypothalamus (Figure 7E-F), males and females differed in the proportion of sex-induced Fos in FG+ cells. For example, in the PeF, females had a higher level of co-localization than males (44% versus 18% in males, Figures 9 and 10). Moderate amounts of Fos/FG+ cells were observed in both males and females in the PVN (Figures 9 and 11) and PH (Figure 9).

In the thalamus (Figure 7E-G) moderate levels of Fos/FG+ co-localization were present in the PrC for males and females. In the PF, females had a greater percentage of Fos/FG+ co-localization than males (16% versus 2%; Figure 9).

Mesencephalon. Representative plots of Fos/FG+ labeling in the mesencephalic regions are shown in Figure 7. In the midbrain (Figure 7G-M), moderate levels of Fos/FG co-localization were observed in the DpMe and InCo in both sexes (Figure 9). Interestingly, while the PAG (Figure 7H-M) contained high levels of both Fos and FG, low levels of co-localization (on average 13%) were observed in both males and females (Figure 12). This was true even though females had significantly higher levels of retrogradely labeled cells (Figure 6A).

High levels of Fos were only present in the outermost layers of the superior and inferior colliculus of both sexes, where retrograde labeling was not observed. Consequently, low to moderate levels of Fos/FG co-localization were observed in the superior and inferior colliculus (Figure 7H-M).

Metencephalon and Myelencephalon. Representative plots of Fos/FG+ labeling in the metencephalic regions are shown in Figure 7K-M and for the myelencephalon in Figure 7N-O. Overall, sex-induced Fos was generally low or absent in both sexes.

Discussion

In this study, we characterized nPGi afferents as to their location, gonadal steroid receptor expression, and activation during sexual behavior. The general anatomical organization of nPGi afferents was similar between the sexes in that there were no regions projecting to the nPGi in only one sex. However, qualitative and quantitative sex differences were observed within specific subregions of the brain (see Figure 13). ER_{α} expression in nPGi afferents was highly variable between the sexes with no consistent pattern overall. Conversely, AR expression in nPGi afferents was almost exclusively higher in males than females. Activation of nPGi afferents during sex was observed throughout the brain in almost all regions that provide dense input to the nPGi, and subregion-specific sex differences in nPGi afferent activation during sex were observed. Sex differences in FG co-localization with ER_{α}, AR, or sex-induced Fos may be reflective of sex differences in basal expression of these proteins in the regions examined. Nevertheless, any sex differences noted in cells projecting to the nPGi have implications for how males and females may sex-specifically regulate genital reflexes. Those regions known to be important to sexual behavior, or that exhibited large sex differences in organization or activity, are discussed below.

Preoptic Area

Our analysis revealed that male rats have significantly more nPGi afferents from the caudal MPO than females, and that these projections contain significantly more AR and sex-induced Fos than females. We also observed that females had more nPGi afferents from the rostral MPO than males, and these projections contained more ER_{α} and sex-induced Fos.

The rostrocaudal difference between the sexes in the relative number of nPGi afferents from the MPO, their gonadal steroid receptor expression, and their activation during sex may represent a fundamental principle in the control of sexual behavior, at least with regards to

genital reflexes. Other studies have underscored the importance of this rostrocaudal MPO distinction with regard to sexual behavior. In male rats, lesions restricted to the caudal MPO disrupt sexual behavior (Van De Poll and Van Dis, 1979), while lesions restricted to the rostral MPO do not effect non-contact erections (a genital reflex) although other aspects of sexual behavior (including ejaculation) are impaired (Liu et al., 1997). In female rats, Fos immunoreactivity by mounts or intromissions alone is induced in ER_{α} expressing rostral, but not caudal preoptic cells (Greco et al., 2003). Our findings are in agreement with this work where nPGi afferents from the rostral MPO have a female-bias in number, ER_{α} expression, and sex-induced Fos. By contrast nPGi afferents from the caudal MPO have a male-bias in number, AR expression, and sex-induced Fos.

A subregion of the caudal MPO in male rats, in the dorsolateral portion of the MPO, near the striohypothalamic nucleus may be critical to the control of genital reflexes in males, but not females, as retrograde labeling in this group of cells is consistently observed in males but not females. Sex-induced Fos was co-localized to a high degree in this region in males. The striohypothalamic nucleus is known to receive projections from the amygdala (Perez-Clausell et al., 1989), and the retrograde labeling we observed may be part of this complex. It is conceivable that projections from the striohypothalamic nucleus inhibit nPGi function upon activation of relevant pheromonal signals processed by the amygdala. Support for this idea comes from work in hamsters where the magnocellular preoptic nucleus, which may be a homologue to the region described here, has been described as part of a BNST-amygdala network that transduces pheromonal signals to sexual behavior motor output (Swann et al., 2003; Wood and Newman, 1995). Furthermore, in male rats, MPO lesions that also encompassed this region produce deficits in the percent of males that mounted, intrommitted, and ejaculated,

during a sexual behavior test (Liu et al., 1997). Work in quail also supports the importance of this subregion of the MPO in male sexual behavior. Although a clear homologue to the quail medial preoptic nucleus (POM) has not been established, the behavioral effects and anatomical connectivity (Balthazart and Ball, 2007; Carere et al., 2007) are similar to the region we describe here. In fact, the dorsolateral portion of the POM appears to be critical for the consummatory aspects of male copulatory behavior in quail (Balthazart et al., 1998). Taken together, the evidence is mounting that this subregion of the MPO is the critical component to male consummatory sexual behavior across species.

In males, the MPO can also affect the nPGi through a relay in the PAG (Murphy et al., 1999a). It is not clear how the projections from the MPO to the nPGi and the MPO to PAG to nPGi work together. We found that MPO efferents to the nPGi were active during sexual behavior, but that PAG afferents to the nPGi were not, despite the large contribution of this region in input to the nPGi. It is possible that the MPO has a pro-sexual effect by inhibiting the nPGi directly, and also by inhibiting PAG cells that normally enhance nPGi activity.

Amygdala / Bed Nucleus of the Stria Terminalis

We observed a greater number of nPGi afferents from the caudal BNST in males than females. These afferents expressed AR to a higher degree in males than females, but expressed ER_{α} similarly in both sexes, and neither sex expressed sex-induced Fos to a large degree. The BNST of rodents is part of a highly interconnected network with the amygdala and MPO where the contextual relevancy of pheromones is determined (Fiber et al., 1993; Kollack-Walker and Newman, 1997; Wood and Newman, 1995). BNST efferents to the nPGi may signal this relevancy, modulating nPGi activity and thereby providing the nPGi external contextual information (i.e. sexual odor vs. food odor). Although we have shown that the caudal portion of

the BNST provides dense input to the nPGi, the majority of these afferents did not express Fos following sexual behavior. These regions may preferentially signal appetitive aspects of sexual behavior to the nPGi, which our sexual behavior model would not have necessarily been able to detect, or alternatively, were inhibited by sexual behavior and therefore would not be expected to show Fos immunoreactivity.

The number of cells projecting from the CeM to the nPGi, their steroid receptor expression, and sex-behavior induced Fos in these cells were similar between the sexes. CeM efferents to the nPGi may be active in other behavioral contexts. For example, the CeM is known to be involved in the processing of stressful stimuli (McEwen, 2007), and CeM-nPGi projections have previously been hypothesized to regulate behavioral defense responses in cats (Hopkins and Holstege, 1978). It is possible that this region, when active during stressful situations, inhibits genital reflexes by enhancing nPGi activity. Interestingly, the amygdala in men is inhibited during ejaculation, as measured by functional magnetic resonance imaging (Holstege et al., 2003), suggesting that its activity may be part of an inhibitory network. The CeM also appears to be part of a genitosensory network. Recent work in our lab using an anterograde trans-neuronal tracer injected into the genitals of male and female rats has found dense anterograde labeling in the central amygdala (Normandin and Murphy, 2007), providing a functional pathway for the modulation of nPGi activity by the CeM through the integration of genitosensory information.

Hypothalamus

The PVN provides dense projections to the nPGi, which show little expression of ER_{α} or AR, and are highly active following sexual activity in both sexes. The robust input to the nPGi from the PVN in, and its associated activity during sexual behavior in, indicates that this region

may be critical in both sexes in the control of genital reflexes in both sexes. The PVN has been previously implicated in sexual behavior. Oxytocin fibers from the PVN are found in the spinal cord regions mediating genital reflexes in male rats (Tang et al., 1998), and there is evidence that the PVN can directly affect motoneuron pools associated with sexual behavior (Perez et al., 2005; Wagner and Clemens, 1991). PVN efferents to the nPGi may inhibit nPGi activity to reduce the overall inhibitory tone to genital reflexes, while at the same time producing direct excitation of spinal motor neurons. Indeed, PVN activity has been associated with both erectile and ejaculatory behavior in male rats (Chen et al., 1997), and both males and females show an increase in Fos immunoreactivity in the PVN following mating (Flanagan et al., 1993; Rowe and Erskine, 1993; Witt and Insel, 1994).

The PeF projections to the nPGi were highly active in females but not males, indicating that this region may be important for sex-specific the control of genital reflexes. This neuropeptide rich region, containing orexin, dynorphin, and neuropeptide W (Nambu et al., 1999; Niimi and Murao, 2005; Zardetto-Smith et al., 1988) has previously been associated with feeding behavior (Sweet et al., 1999), as well as arousal (Suntsova et al., 2007; Uschakov et al., 2006) and suggests that this nucleus may be part of a general motivational circuit. Interestingly, the PeF has also been implicated as part of the dopaminergic system of rats, as it projects heavily to dopaminergic neurons of the VTA (Fadel and Deutch, 2002), suggesting a role of the PeF in reward/reinforcement systems. In fact, at least in males, systemic orexin antagonsists impair copulation (Muschamp et al., 2007). Furthermore, orexin-A administration increases the firing rate of VTA cells, and tyrosine hydroxylase-positive VTA cells also express mating-induced Fos and are in close apposition to orexinergic fibers (Muschamp et al., 2007). Presumably, PeF

activity would also inhibit nPGi function, enabling pro-sexual behavior, and our data suggests that PeF signaling to the nPGi may be more important in females.

PAG

Throughout the rostrocaudal extent of the PAG, there were significantly more retrogradely labeled cells in females in comparison to males. Co-localization with ER_{α} was comparable between the sexes while AR expression in these cells was greater in males than females at all levels examined. Sex differences in PAG output to the brainstem have been previously reported (Loyd and Murphy, 2006), and suggest an overarching principle of PAG-brainstem organization whereby females in general have a larger number of output neurons utilized in a specific circuit than males. Given the large population of gonadal steroid receptors localized within the PAG (Murphy et al., 1999b), these observed sex differences could be due to circulating gonadal steroids during a critical period or alternatively, represent plasticity within the female PAG due to changes in gonadal steroid levels across the estrous cycle (Griffiths and Lovick, 2005).

In males, PAG neurons that project to the nPGi are preferentially localized within regions receiving input from the MPO (Murphy and Hoffman, 2001). For example, there are no projections from the MPO to the dorsolateral PAG; similarly, no PAG-nPGi output neurons are located there, suggesting there is an MPO-PAG-nPGi circuit. In addition to receiving input from the MPO, PAG-nPGi output neurons also receive direct input from the lumbosacral spinal cord (unpublished observations), thereby forming a unique spinal-supraspinal-spinal circuit. Interestingly, while sexual behavior induced extensive Fos within the PAG of both males and females, very little Fos was observed in PAG-nPGi output neurons, suggesting that these neurons were not directly excited during sexual behavior. Rather, the finding of little Fos expression in

PAG-nPGi output neurons suggests that these neurons may actually have been inhibited during sex; given that nPGi-spinal cord pathway must be disinhibited for genital reflexes to occur, it is intriguing to consider the possibility that PAG output to the nPGi is the source of disinhibition. The PAG receives chemosensory and neuroendocrine input, as well as sensory information pertaining to the exterior environment. Together, this suggests that the PAG may function as the primary 'decision maker' as to whether the intrinsic and extrinsic environment is appropriate for mating to occur. If the conditions are appropriate for mating, inhibitory drive from the PAG to the nPGi is initiated and the tonic inhibition over nPGi-spinal cord is removed. In addition, excitatory drive to the nPGi from the MPO is initiated (reflected in the high percentage of Fos in MPO-nPGi neurons) and mating occurs. Obviously, this is highly speculative and requires additional testing to evaluate these hypotheses.

Superior and Inferior Colliculus

Females had a greater number of collicular cells projecting to the nPGi than males; moderate amounts of sex-induced Fos were observed. The superior colliculus is classically described as part of the circuit producing saccades in mammalian systems. However, recent evidence suggests that the superior colliculus may also be described as a source of attentional modulation for goal directed behavior that is independent of specific motor output (Krauzlis et al., 2004). Stimulation of the deep layers of the superior colliculus, the same region where the majority of afferent contributions to the nPGi are located, results in increased attentiveness in rats (Schenberg et al., 2005). In addition, we found that the PrC of the thalamus projects heavily to the nPGi, and this region is known to be connected to areas governing attention, including the superior colliculus (Canteras and Goto, 1999). The activity of superior collicular/PrC projections

to the nPGi may modulate nPGi function based on specific goal directed behaviors, such as mate pursuit and proceptive sexual behaviors.

Like the superior colliculus, females had a greater number of inferior collicular cells projecting to the nPGi than males; moderate amounts of sex-induced Fos were observed. The inferior colliculus is a part of the auditory system (Brozoski et al., 2007; Sun et al., 2007), and inferior collicular input to the nPGi may function to integrate auditory signals into sexual behavior output. Both male and female rats produce ultrasonic vocalizations during sexual behavior (McGinnis and Vakulenko, 2003), and detection of these signals has the potential to modulate sexual behavior in rodents (Floody et al., 1998; Floody and Lisk, 1987; McGinnis and Vakulenko, 2003). The relative difference between male and female rats in inferior collicular projections to the nPGi may indicate a difference in the importance of these ultrasonic vocalizations to the animals behavioral output. Indeed females show higher levels of activity in the midbrain when listening to simulated mating-like ultrasonic vocalizations (Floody and Lisk, 1987).

The nPGi as a central integrator for arousal

While we have focused on the role of the nPGi in sexual behavior, the nPGi has been implicated in a variety of seemingly disparate systems including blood pressure (Lovick, 1992), respiration (Saether et al., 1987), nociception (Lanteri-Minet et al., 1994), reinforcement (Fathi-Moghaddam et al., 2006), audition (Kandler and Herbert, 1991) *and* sexual behavior (Yells et al., 1992). Collectively, these behavioral domains all contain an arousal component, and the nPGi may be one brainstem region that integrates a multitude of inputs modulating arousal in these behavioral systems (Van Bockstaele and Aston-Jones, 1995).

Anatomical data support this hypothesized "integrator" role of the nPGi. Descending projections from the nPGi to spinal cell groups outside of those devoted to the somatic component of genital reflexes have been noted, including the intermediolateral cell column and the sacral parasympathetic nucleus (Hermann et al., 2003; Holstege et al., 1979). In addition, the nPGi projects to the LC in rats (Aston-Jones et al., 1986; Luppi et al., 1995), and this nPGi-LC pathway has been implicated in a number of arousal-dependant functions (Chen and Engberg, 1989; Clark and Proudfit, 1991; Clayton and Williams, 2000). The widespread afferents to the nPGi observed in the present study, in conjunction with nPGi output to sympathetic and parasympathetic neurons, and a supraspinal noradrenergic center, are one obvious way the nPGi can be seen as a stimulus integrator for arousal modulation in rats. The nPGi receives extensive input from the PAG, a region known to regulate "fight or flight" responses (Carrive et al., 1987; Misslin, 2003), lending further support to this idea. The regulation of arousal by the nPGi may be sexually dimorphic, at least with respect to the information generated by the PAG, as we observed a greater number of nPGi afferents from the PAG in females.

In addition to these regions classically associated with arousal, the auditory system inputs to the nPGi from the cochlear nucleus and inferior colliculus may represent an integration of important auditory cues for generating changes in arousal as well. The nPGi receives input from the cochlear nucleus (Bellintani-Guardia et al., 1996), an auditory processing center, and we observed significant input from the inferior colliculus in both sexes. Lesions of the inferior colliculus produce an increase in startle responses to an auditory stimuli (Leitner and Cohen, 1985), suggesting a loss of behavioral inhibition that could be mediated by the nPGi. Pontine regions are known to produce inhibition of the startle reflex (Fendt et al., 2001), and we have observed that many of the regions associated with this regulatory role (PPTg, LDTg, SNR)

project to the nPGi. As females had a greater number of cells in the inferior colliculus that projected to the nPGi than males, this suggests that the regulation of arousal by auditory stimulation may be sexually dimorphic.

Summary

The results of this study indicate that both male and female rats have extensive projections to the nPGi throughout the brain. Some of these nPGi-projecting regions, such as the PAG, superior colliculus, and inferior colliculus, show a significant female-biased sex difference in the relative number of cells projecting to the nPGi. In the MPO, however, we observed a significant male-biased sex-difference in the relative number of cells projecting to the nPGi. Throughout the brain nPGi afferents contained receptors for the gonadal steroids, suggesting that changes in hormone levels during sexual behavior, or across the estrous cycle, may modulate the excitability of nPGi afferents. ER_{α} is expressed in many nPGi afferents in both sexes almost equally with few exceptions. AR is also expressed in nPGi afferents of both sexes, with a clear male-bias in many regions, significantly so in the PAG. Many of these nPGi afferents are activated during sexual behavior, though a minority do so to a large degree.

Our characterization of the anatomical organization, gonadal steroid receptor expression, and activity during sexual behavior of nPGi afferents is another step in understanding the control of genital reflexes. Our analysis provides a new insight into the regulation of genital reflexes by supraspinal sites. The number and variety of nPGi afferents suggest that the nPGi itself is a major integrator of signals relevant to the production of genital reflexes. This integration is likely to be context dependant as brain regions implicated in sexual behavior, stress, arousal, audition and attention provide input to the nPGi. Our analysis reveals that this integration is

sexually dimorphic, possibly reflecting a bias in the importance of particular signals sent to the nPGi for appropriate genital reflex function. This information advances the understanding of the basic principles underlying human sexual dysfunction as it pertains to the supraspinal regulation of genital reflexes, and provides targets for further study.

Acknowledgments

The authors would like to acknowledge the technical assistance of Ryan Castaneira and Tayisha Vilceus.

Literature Cited

Aston-Jones G, Ennis M, Pieribone VA, Nickell WT, Shipley MT. 1986. The brain nucleus locus coeruleus: restricted afferent control of a broad efferent network. Science 234(4777):734-737.

Balthazart J, Absil P, Gerard M, Appeltants D, Ball GF. 1998. Appetitive and consummatory male sexual behavior in Japanese quail are differentially regulated by subregions of the preoptic medial nucleus. J Neurosci 18(16):6512-6527.

Balthazart J, Ball GF. 2007. Topography in the preoptic region: Differential regulation of appetitive and consummatory male sexual behaviors. Front Neuroendocrinol.

Bellintani-Guardia B, Schweizer M, Herbert H. 1996. Analysis of projections from the cochlear nucleus to the lateral paragigantocellular reticular nucleus in the rat. Cell Tissue Res 283(3):493-505.

Brozoski TJ, Ciobanu L, Bauer CA. 2007. Central neural activity in rats with tinnitus evaluated with manganese-enhanced magnetic resonance imaging (MEMRI). Hearing research 228(1-2):168-179.

Cameron A, Tomlin M. 2007. The effect of male erectile dysfunction on the psychosocial, relationship, and sexual characteristics of heterosexual women in the United States. J Sex Marital Ther 33(2):135-149.

Canteras NS, Goto M. 1999. Connections of the precommissural nucleus. J Comp Neurol 408(1):23-45.

Carere C, Ball GF, Balthazart J. 2007. Sex differences in projections from preoptic area aromatase cells to the periaqueductal gray in Japanese quail. J Comp Neurol 500(5):894-907.

Carrive P, Dampney RA, Bandler R. 1987. Excitation of neurones in a restricted portion of the midbrain periaqueductal grey elicits both behavioural and cardiovascular components of the defence reaction in the unanaesthetised decerebrate cat. Neurosci Lett 81(3):273-278.

Chen KK, Chan SH, Chang LS, Chan JY. 1997. Participation of paraventricular nucleus of hypothalamus in central regulation of penile erection in the rat. The Journal of urology 158(1):238-244.

Chen Z, Engberg G. 1989. The rat nucleus paragigantocellularis as a relay station to mediate peripherally induced central effects of nicotine. Neurosci Lett 101(1):67-71.

Clark FM, Proudfit HK. 1991. Projections of neurons in the ventromedial medulla to pontine catecholamine cell groups involved in the modulation of nociception. Brain Res 540(1-2):105-115.

Clayton EC, Williams CL. 2000. Posttraining inactivation of excitatory afferent input to the locus coeruleus impairs retention in an inhibitory avoidance learning task. Neurobiol Learn Mem 73(2):127-140.

Creutz LM, Kritzer MF. 2004. Mesostriatal and mesolimbic projections of midbrain neurons immunoreactive for estrogen receptor beta or androgen receptors in rats. J Comp Neurol 476(4):348-362.

Fadel J, Deutch AY. 2002. Anatomical substrates of orexin-dopamine interactions: lateral hypothalamic projections to the ventral tegmental area. Neuroscience 111(2):379-387.

Fathi-Moghaddam H, Kesmati M, Kargar HM. 2006. The effect of paragigantocellularis lateralis lesion on conditioned place preference (CPP) in presence or absence of alpha2 adrenergic agonist (clonidine) in male rats. Acta Physiol Hung 93(1):33-40.

Fendt M, Li L, Yeomans JS. 2001. Brain stem circuits mediating prepulse inhibition of the startle reflex. Psychopharmacology 156(2-3):216-224.

Fiber JM, Adames P, Swann JM. 1993. Pheromones induce c-fos in limbic areas regulating male hamster mating behavior. Neuroreport 4(7):871-874.

Flanagan LM, Pfaus JG, Pfaff DW, McEwen BS. 1993. Induction of FOS immunoreactivity in oxytocin neurons after sexual activity in female rats. Neuroendocrinology 58(3):352-358.

Floody OR, Cooper TT, Albers HE. 1998. Injection of oxytocin into the medial preoptic-anterior hypothalamus increases ultrasound production by female hamsters. Peptides 19(5):833-839.

Floody OR, Lisk RD. 1987. Effects of sex and reproductive state on acoustic responsiveness in hamsters. Brain research bulletin 18(2):235-244.

Greco B, Blasberg ME, Kosinski EC, Blaustein JD. 2003. Response of ERalpha-IR and ERbeta-IR cells in the forebrain of female rats to mating stimuli. Hormones and behavior 43(4):444-453.

Griffiths JL, Lovick TA. 2005. GABAergic neurones in the rat periaqueductal grey matter express alpha4, beta1 and delta GABAA receptor subunits: plasticity of expression during the estrous cycle. Neuroscience 136(2):457-466.

Hermann GE, Holmes GM, Rogers RC, Beattie MS, Bresnahan JC. 2003. Descending spinal projections from the rostral gigantocellular reticular nuclei complex. J Comp Neurol 455(2):210-221.

Holmes GM, Chapple WD, Leipheimer RE, Sachs BD. 1991. Electromyographic analysis of male rat perineal muscles during copulation and reflexive erections. Physiol Behav 49(6):1235-1246.

Holstege G, Georgiadis JR, Paans AM, Meiners LC, van der Graaf FH, Reinders AA. 2003. Brain activation during human male ejaculation. J Neurosci 23(27):9185-9193.

Holstege G, Kuypers HG, Boer RC. 1979. Anatomical evidence for direct brain stem projections to the somatic motoneuronal cell groups and autonomic preganglionic cell groups in cat spinal cord. Brain Res 171(2):329-333.

Hopkins DA, Holstege G. 1978. Amygdaloid projections to the mesencephalon, pons and medulla oblongata in the cat. Exp Brain Res 32(4):529-547.

Johnson RD, Hubscher CH. 1998. Brainstem microstimulation differentially inhibits pudendal motoneuron reflex inputs. Neuroreport 9(2):341-345.

Kandler K, Herbert H. 1991. Auditory projections from the cochlear nucleus to pontine and mesencephalic reticular nuclei in the rat. Brain Res 562(2):230-242.

Kollack-Walker S, Newman SW. 1997. Mating-induced expression of c-fos in the male Syrian hamster brain: role of experience, pheromones, and ejaculations. Journal of neurobiology 32(5):481-501.

Krauzlis RJ, Liston D, Carello CD. 2004. Target selection and the superior colliculus: goals, choices and hypotheses. Vision research 44(12):1445-1451.

Lanteri-Minet M, Weil-Fugazza J, de Pommery J, Menetrey D. 1994. Hindbrain structures involved in pain processing as revealed by the expression of c-Fos and other immediate early gene proteins. Neuroscience 58(2):287-298.

Laumann EO, Paik A, Rosen RC. 1999. Sexual dysfunction in the United States: prevalence and predictors. JAMA 281(6):537-544.

Lee JW, Erskine MS. 2000. Pseudorabies virus tracing of neural pathways between the uterine cervix and CNS: effects of survival time, estrogen treatment, rhizotomy, and pelvic nerve transection. J Comp Neurol 418(4):484-503.

Leitner DS, Cohen ME. 1985. Role of the inferior colliculus in the inhibition of acoustic startle in the rat. Physiol Behav 34(1):65-70.

Liu YC, Sachs BD. 1999. Erectile function in male rats after lesions in the lateral paragigantocellular nucleus. Neurosci Lett 262(3):203-206.

Liu YC, Salamone JD, Sachs BD. 1997. Lesions in medial preoptic area and bed nucleus of stria terminalis: differential effects on copulatory behavior and noncontact erection in male rats. J Neurosci 17(13):5245-5253.

Lovick TA. 1986. Projections from brainstem nuclei to the nucleus paragigantocellularis lateralis in the cat. J Auton Nerv Syst 16(1):1-11.

Lovick TA. 1992. Midbrain influences on ventrolateral medullo-spinal neurones in the rat. Exp Brain Res 90(1):147-152.

Loyd DR, Murphy AZ. 2006. Sex differences in the anatomical and functional organization of the periaqueductal gray-rostral ventromedial medullary pathway in the rat: a potential circuit mediating the sexually dimorphic actions of morphine. J Comp Neurol 496(5):723-738.

Luppi PH, Aston-Jones G, Akaoka H, Chouvet G, Jouvet M. 1995. Afferent projections to the rat locus coeruleus demonstrated by retrograde and anterograde tracing with cholera-toxin B subunit and Phaseolus vulgaris leucoagglutinin. Neuroscience 65(1):119-160.

Madeira MD, Leal S, Paula-Barbosa MM. 1999. Stereological evaluation and Golgi study of the sexual dimorphisms in the volume, cell numbers, and cell size in the medial preoptic nucleus of the rat. Journal of neurocytology 28(2):131-148.

Marson L. 1995. Central nervous system neurons identified after injection of pseudorabies virus into the rat clitoris. Neurosci Lett 190(1):41-44.

Marson L, Cai R, Makhanova N. 2003. Identification of spinal neurons involved in the urethrogenital reflex in the female rat. J Comp Neurol 462(4):355-370.

Marson L, Foley KA. 2004. Identification of neural pathways involved in genital reflexes in the female: a combined anterograde and retrograde tracing study. Neuroscience 127(3):723-736.

Marson L, List MS, McKenna KE. 1992. Lesions of the nucleus paragigantocellularis alter ex copula penile reflexes. Brain Res 592(1-2):187-192.

Marson L, Murphy AZ. 2006. Identification of neural circuits involved in female genital responses in the rat: a dual virus and anterograde tracing study. American journal of physiology 291(2):R419-428.

McEwen BS. 2007. Physiology and neurobiology of stress and adaptation: central role of the brain. Physiological reviews 87(3):873-904.

McGinnis MY, Vakulenko M. 2003. Characterization of 50-kHz ultrasonic vocalizations in male and female rats. Physiol Behav 80(1):81-88.

McKenna KE, Nadelhaft I. 1986. The organization of the pudendal nerve in the male and female rat. J Comp Neurol 248(4):532-549.

Misslin R. 2003. The defense system of fear: behavior and neurocircuitry. Neurophysiol Clin 33(2):55-66.

Murphy AZ, Hoffman GE. 2001. Distribution of gonadal steroid receptor-containing neurons in the preoptic-periaqueductal gray-brainstem pathway: a potential circuit for the initiation of male sexual behavior. J Comp Neurol 438(2):191-212.

Murphy AZ, Marson L. 2000. Identification of neural circuits underlying male reproductive behavior: combined viral and traditional tract tracing studies. Annual Meeting of the Society for Neuroscience. New Orleans, LA.

Murphy AZ, Rizvi TA, Ennis M, Shipley MT. 1999a. The organization of preoptic-medullary circuits in the male rat: evidence for interconnectivity of neural structures involved in reproductive behavior, antinociception and cardiovascular regulation. Neuroscience 91(3):1103-1116.

Murphy AZ, Shupnik MA, Hoffman GE. 1999b. Androgen and estrogen (alpha) receptor distribution in the periaqueductal gray of the male Rat. Hormones and behavior 36(2):98-108.

Muschamp JW, Dominguez JM, Sato SM, Shen RY, Hull EM. 2007. A role for hypocretin (orexin) in male sexual behavior. J Neurosci 27(11):2837-2845.

Nambu T, Sakurai T, Mizukami K, Hosoya Y, Yanagisawa M, Goto K. 1999. Distribution of orexin neurons in the adult rat brain. Brain Res 827(1-2):243-260.

Niimi M, Murao K. 2005. Neuropeptide W as a stress mediator in the hypothalamus. Endocrine 27(1):51-54.

Normandin JJ, Murphy AZ. 2007. Feeling good in the neighborhood: trans-synpatic tracing of genitosensory afferents. Annual Meeting of the Society for Behavioral Neuroendocrinology. Pacific Grove, CA.

Paxinos G, Watson C. 1997. The Rat Brain in Stereotaxic Coordinates. San Diego: Academic Press.

Perez-Clausell J, Frederickson CJ, Danscher G. 1989. Amygdaloid efferents through the stria terminalis in the rat give origin to zinc-containing boutons. J Comp Neurol 290(2):201-212.

Perez CA, Concha A, Hernandez ME, Manzo J. 2005. Influence of the paraventricular nucleus and oxytocin on the retrograde stain of pubococcygeus muscle motoneurons in male rats. Brain Res 1041(1):11-18.

Pfaus JG. 1996. Frank A. Beach award. Homologies of animal and human sexual behaviors. Hormones and behavior 30(3):187-200.

Quesada A, Romeo HE, Micevych P. 2007. Distribution and localization patterns of estrogen receptor-beta and insulin-like growth factor-1 receptors in neurons and glial cells of the female rat substantia nigra: localization of ERbeta and IGF-1R in substantia nigra. J Comp Neurol 503(1):198-208.

Rowe DW, Erskine MS. 1993. c-Fos proto-oncogene activity induced by mating in the preoptic area, hypothalamus and amygdala in the female rat: role of afferent input via the pelvic nerve. Brain Res 621(1):25-34.

Saether K, Hilaire G, Monteau R. 1987. Dorsal and ventral respiratory groups of neurons in the medulla of the rat. Brain Res 419(1-2):87-96.

Schenberg LC, Povoa RM, Costa AL, Caldellas AV, Tufik S, Bittencourt AS. 2005. Functional specializations within the tectum defense systems of the rat. Neuroscience and biobehavioral reviews 29(8):1279-1298.

Sun X, Xia Q, Lai CH, Shum DK, Chan YS, He J. 2007. Corticofugal modulation of acoustically induced Fos expression in the rat auditory pathway. J Comp Neurol 501(4):509-525.

Suntsova N, Guzman-Marin R, Kumar S, Alam MN, Szymusiak R, McGinty D. 2007. The median preoptic nucleus reciprocally modulates activity of arousal-related and sleep-related neurons in the perifornical lateral hypothalamus. J Neurosci 27(7):1616-1630.

Swann JM, Wang J, Govek EK. 2003. The MPN mag: introducing a critical area mediating pheromonal and hormonal regulation of male sexual behavior. Annals of the New York Academy of Sciences 1007:199-210.

Sweet DC, Levine AS, Billington CJ, Kotz CM. 1999. Feeding response to central orexins. Brain Res 821(2):535-538.

Tang Y, Rampin O, Calas A, Facchinetti P, Giuliano F. 1998. Oxytocinergic and serotonergic innervation of identified lumbosacral nuclei controlling penile erection in the male rat. Neuroscience 82(1):241-254.

Tang Y, Rampin O, Giuliano F, Ugolini G. 1999. Spinal and brain circuits to motoneurons of the bulbospongiosus muscle: retrograde transneuronal tracing with rabies virus. J Comp Neurol 414(2):167-192.

Uschakov A, Gong H, McGinty D, Szymusiak R. 2006. Sleep-active neurons in the preoptic area project to the hypothalamic paraventricular nucleus and perifornical lateral hypothalamus. The European journal of neuroscience 23(12):3284-3296.

Van Bockstaele EJ, Aston-Jones G. 1995. Integration in the ventral medulla and coordination of sympathetic, pain and arousal functions. Clin Exp Hypertens 17(1-2):153-165.

Van De Poll NE, Van Dis H. 1979. The effect of medial preoptic--anterior hypothalamic lesions on bisexual behavior of the male rat. Brain research bulletin 4(4):505-511.

Wagner CK, Clemens LG. 1991. Projections of the paraventricular nucleus of the hypothalamus to the sexually dimorphic lumbosacral region of the spinal cord. Brain Res 539(2):254-262.

Watson RE, Jr., Wiegand SJ, Clough RW, Hoffman GE. 1986. Use of cryoprotectant to maintain long-term peptide immunoreactivity and tissue morphology. Peptides 7(1):155-159.

Witt DM, Insel TR. 1994. Increased Fos expression in oxytocin neurons following masculine sexual behavior. J Neuroendocrinol 6(1):13-18.

Wood RI, Newman SW. 1995. Integration of chemosensory and hormonal cues is essential for mating in the male Syrian hamster. J Neurosci 15(11):7261-7269.

Yells DP, Hendricks SE, Prendergast MA. 1992. Lesions of the nucleus paragigantocellularis: effects on mating behavior in male rats. Brain Res 596(1-2):73-79.

Yells DP, Prendergast MA, Hendricks SE, Nakamura M. 1994. Fluoxetine-induced inhibition of male rat copulatory behavior: modification by lesions of the nucleus paragigantocellularis. Pharmacol Biochem Behav 49(1):121-127.

Zardetto-Smith AM, Moga MM, Magnuson DJ, Gray TS. 1988. Lateral hypothalamic dynorphinergic efferents to the amygdala and brainstem in the rat. Peptides 9(5):1121-1127.

Legends

Figure 1. Photomicrograph depicting a typical Fluorogold (FG) injection in the nucleus paragigantocellularis (nPGi) of the male (A) and female (B) rat. Note that FG injections are centered in the nPGi with little spread to surrounding regions. 4V=4th ventricle, py=pyramidal tract. Scale bar = 200 µm in A (applies to A, B).

Figure 2. Plots of FG+ cells retrogradely labeled from the nPGi (black: ipsilateral to injection site, gray: solely contralateral to injection site). Also plotted are FG+ cells containing estrogen receptor alpha (ER_α; pink), or androgen receptor (AR; blue) of a representative male (left side) and female (right side) rat in all sections examined, relative to Bregma.

Figure 3. Mean number (± standard error of the mean (SEM)) of FG+ cells retrogradely labeled from the nPGi for four rostrocaudal levels of the medial preoptic area (MPO; A). The mean percentage (± SEM) of FG+ cells that also contained ER_α (B) or AR (C) is also shown. Numbers below atlas images are millimeters relative to Bregma. Note that females have a higher number of FG+ cells in the rostral MPO, whereas males have a higher number of FG+ cells in the caudal MPO. Also note that females have a higher proportion of ER_α/FG+ in the rostral-most level, whereas males have a higher proportion of ER_α/FG+ cells in a caudal level. A higher proportion of AR/FG+ cells at all levels of the MPO were observed in males. * = significant male/female difference, $p \leq 0.05$; MPO=medial preoptic area.

Figure 4. Mean number (± SEM) of FG+ cells retrogradely labeled from the nPGi in all regions with where dense labeling was observed (A). Mean percentage (± SEM) of FG+ cells that also

contained ER_α (B) or AR (C) are also shown. Note the regional specificity in sex differences in FG+ cells. Also note the similarity between the sexes in the proportion of ER_α/FG+ cells, but the male-bias at almost all levels with respect to the proportion of AR/FG+ cells. * = significant male/female difference, $p \leq 0.0031$; r/cBNST= rostral/caudal bed nucleus of the stria terminalis, CeM=central amygdala, PVN=paraventricular nucleus, PH=posterior hypothalamus, PeF=perifornical nucleus, PrC=precommissural nucleus, PF=parafascicular thalamic nucleus, DpMe=deep mesencephalic nucleus, InCo=intercollicular nucleus, rSC=rostral superior colliculus, DpG=deep gray layer of the superior colliculus, ECIC=external cortex of the inferior colliculus, m5=motor root of the trigeminal nerve, LRt=lateral reticular nucleus, Sp5I=interpolar spinal trigeminal nucleus

Figure 5. Photomicrograph of a representative section of the paraventricular nucleus (PVN) in a male (A and C) and female (B and D) rat. C and D are higher magnifications of the area indicated by the box. Neurons stained brown contain FG retrogradely labeled from the nPGi, nuclei stained black contain AR and neurons stained brown with nuclei stained black contain both FG and AR. Note that both males and females have a similar high density of retrogradely labeled cells, and that some of these cells contain AR. Scale bars = 100 μm in A (applies to A, B); 50 μm in C (applies to C, D).

Figure 6. Mean number (± SEM) of FG+ cells retrogradely labeled from the nPGi for six rostrocaudal levels of the periaqueductal gray (PAG; A). The mean percentage (± SEM) of FG+ cells that also contained ER_α (B) or AR (C) is also shown. Numbers below atlas images are millimeters relative to Bregma. Note that females have a higher number of FG labeled cells

throughout the PAG, most notably in the dorsomedial subdivision of the PAG, and that females differed from males significantly at four rostrocaudal levels. Also note that males have a higher proportion of ER_{α}/FG+ or AR/FG+ cells at almost all levels. * = significant male/female difference, $p \leq 0.05$

Figure 7. Plots of FG+ cells retrogradely labeled from the nPGi (black: ipsilateral to injection site; gray: solely contralateral to injection site), and FG+ cells also containing Fos (green) of representative male (left sides) and female (right side) rat in all sections examined.

Figure 8. Mean proportion (± SEM) of FG+ cells retrogradely labeled from the nPGi that also contain sex-induced Fos for four rostrocaudal levels of the MPO. Numbers below atlas images are millimeters relative to Bregma. Note that females have a higher proportion of Fos/FG+ cells in rostral MPO levels, and that males have a higher proportion of Fos/FG+ cells in caudal MPO levels. * = significant male/female difference, $p \leq 0.05$.

Figure 9. Mean proportion (± SEM) of FG+ cells that also contain sex-induced Fos in all regions with dense input to the nPGi. Note the regional specificity in sex differences in the proportion of Fos/FG+, and that only a few regions show high sex-induced Fos in projections to the nPGi. No differences reached significance at the $\alpha \leq 0.0031$ level.

Figure 10. Photomicrograph of a representative section of the perifornical nucleus (PeF) of the hypothalamus in a male (A and C) and female (B and D) rat. C and D are higher magnifications of the area indicated by the box. Neurons stained brown contain FG retrogradely labeled from

the nPGi, nuclei stained black contain sex-induced Fos, and neurons stained brown with nuclei stained black are retrogradely labeled FG cells that also contain sex-induced Fos. Note that females have a higher proportion of FG labeled cells that also contain sex-induced Fos. Scale bars = 100 μm in A (applies to A, B); 50 μm in C (applies to C, D).

Figure 11. Photomicrograph of a representative section of the PVN in a male (A and C) and female (B and D) rat. C and D are higher magnifications of the area indicated by the box. Neurons stained brown contain FG retrogradely labeled from the nPGi, nuclei stained black contain sex-induced Fos, and neurons stained brown with nuclei stained black contain both FG and Fos. Note that both males and females have a similar high density of retrogradely labeled cells, and that many of these cells contain sex-induced Fos. Scale bars = 100 μm in A (applies to A, B); 50 μm in C (applies to C, D).

Figure 12. Mean proportion (± SEM) of FG+ cells retrogradely labeled from the nPGi that also contain sex-induced Fos for six rostrocaudal levels of the PAG. Numbers below atlas images are millimeters relative to Bregma. Male, dark gray; female, light gray. Note that in both sexes the proportion of Fos/FG+ cells is quite low. No differences reached significance at the $\alpha \leq 0.05$ level.

Figure 13. Summary diagram of regions that provide dense input to the nPGi in male (A) and female (B) rats. The color and length of bars adjacent to labels represent the relative density of FG labeled cells that also contain ER_{α} (pink), AR (blue), or sex-induced Fos (green) in those regions.

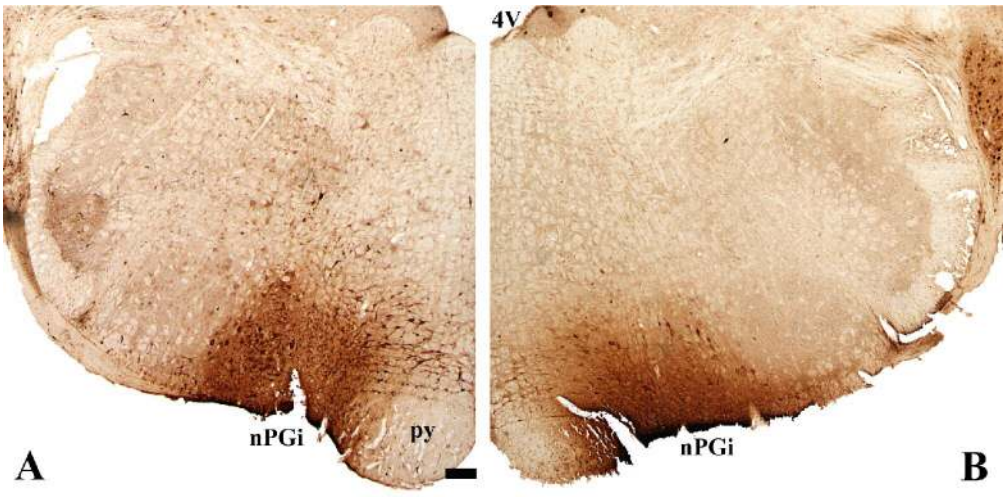

172x85mm (300 x 300 DPI)

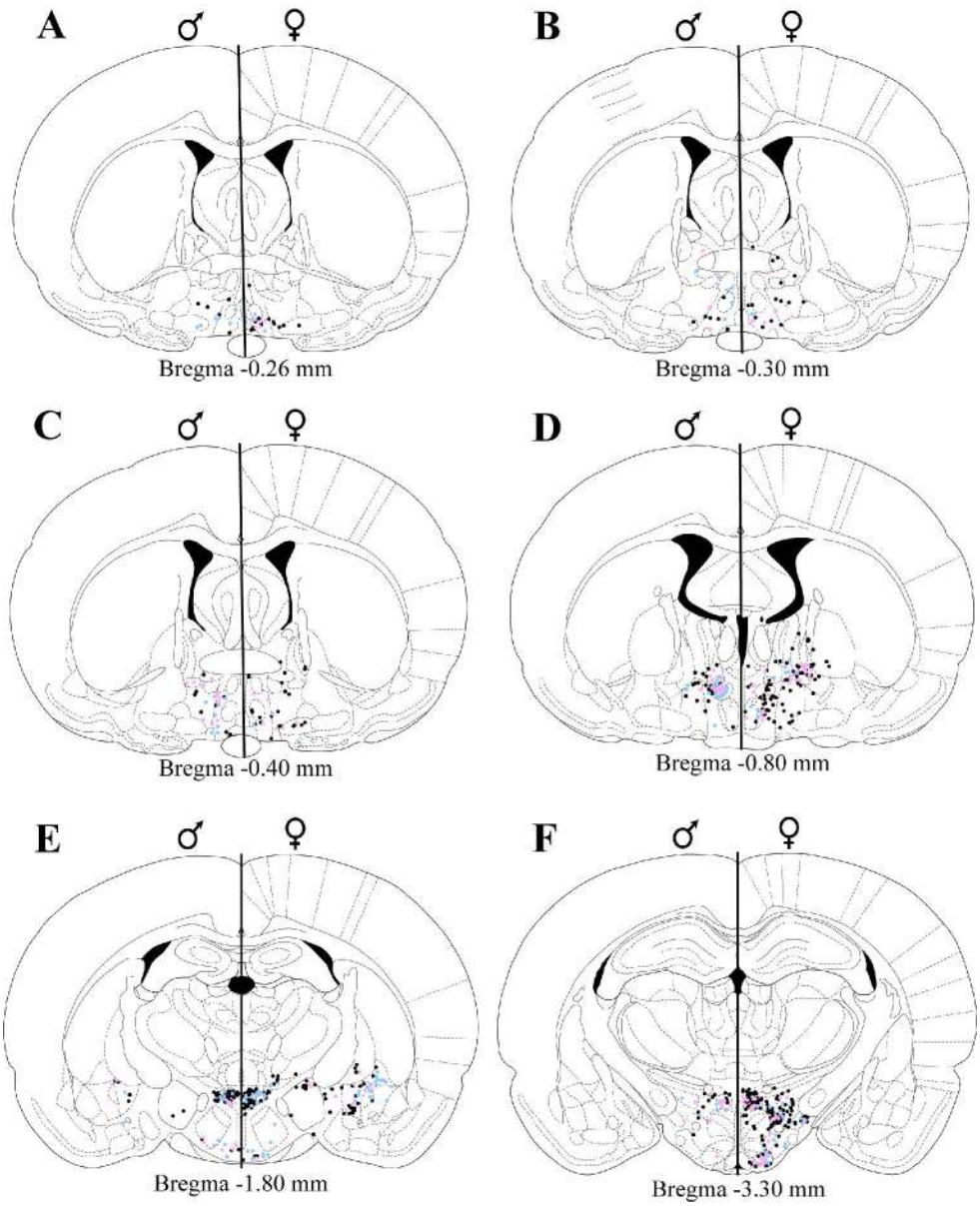

172x212mm (300 x 300 DPI)

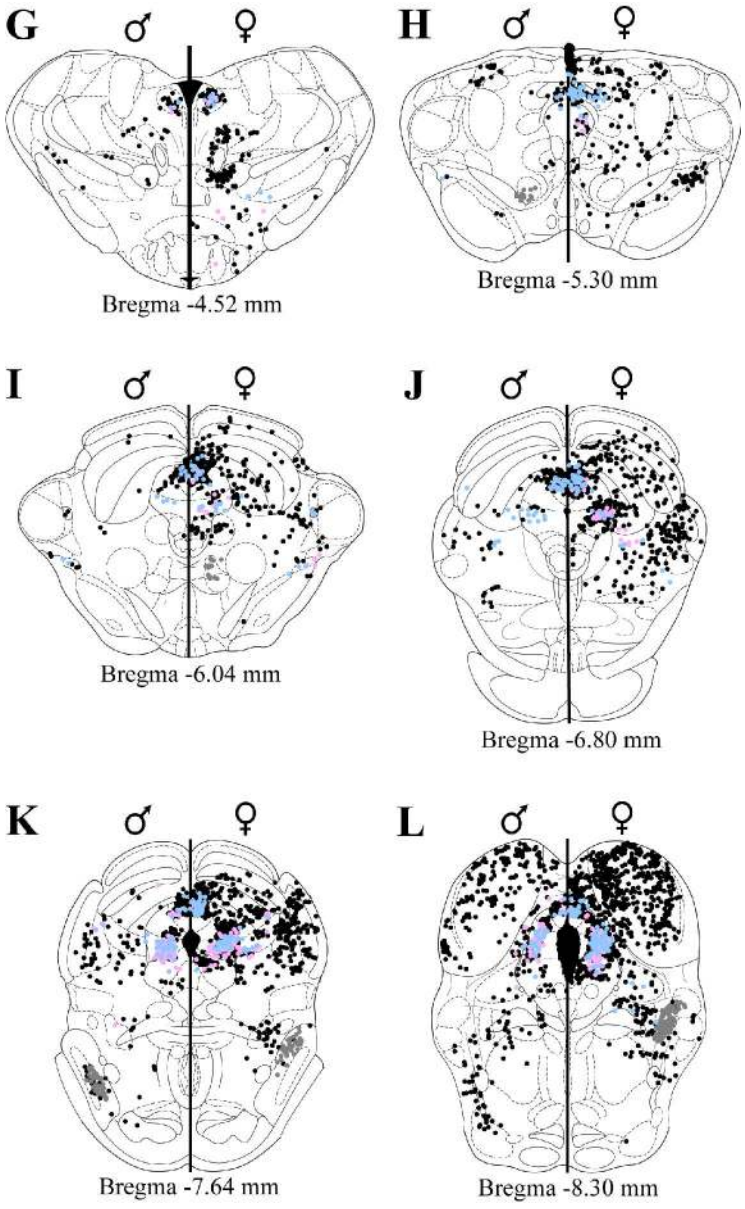

126x205mm (300 x 300 DPI)

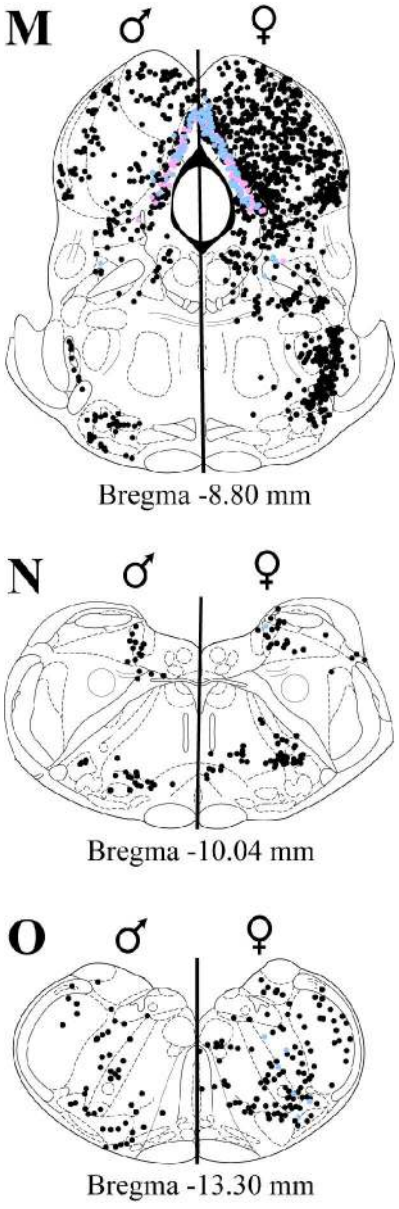

56x173mm (300 x 300 DPI)

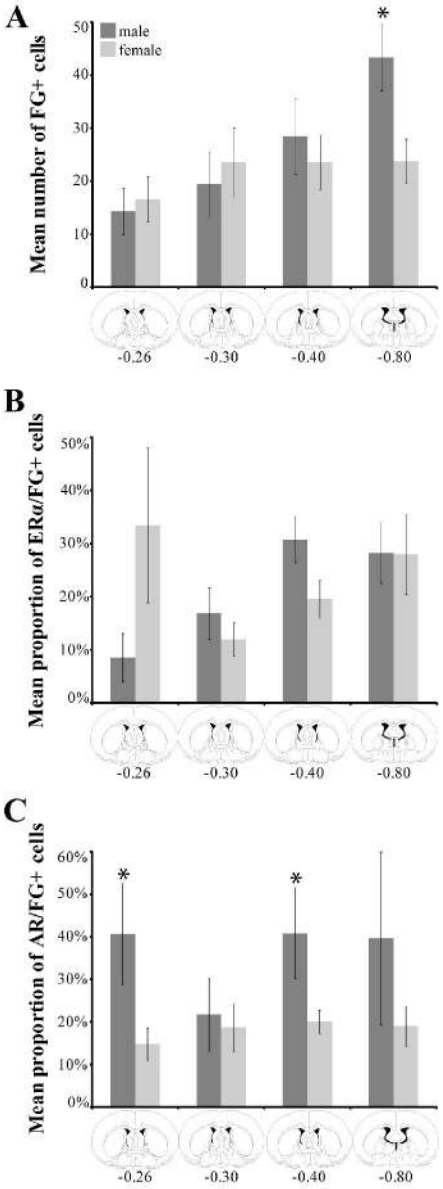

83x227mm (300 x 300 DPI)

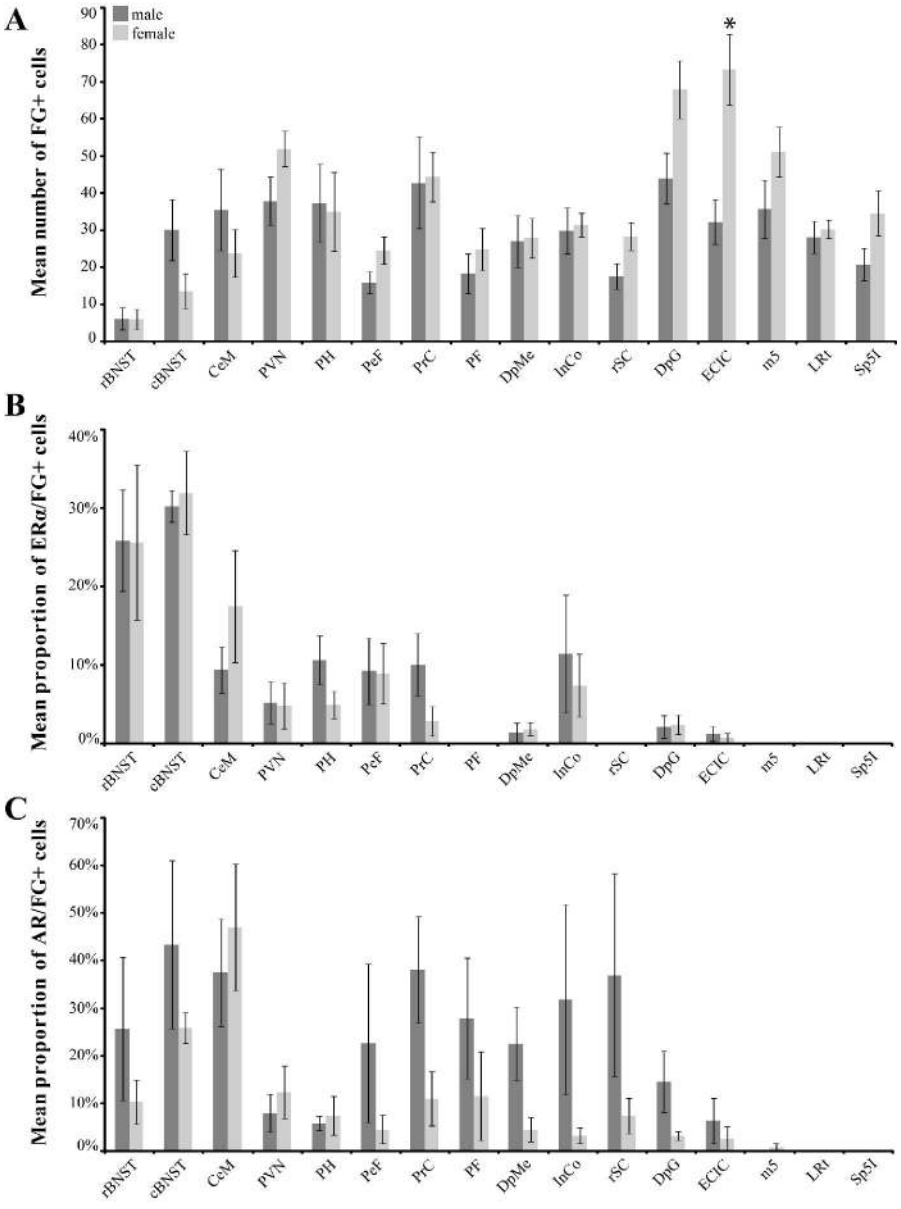

171x231mm (300 x 300 DPI)

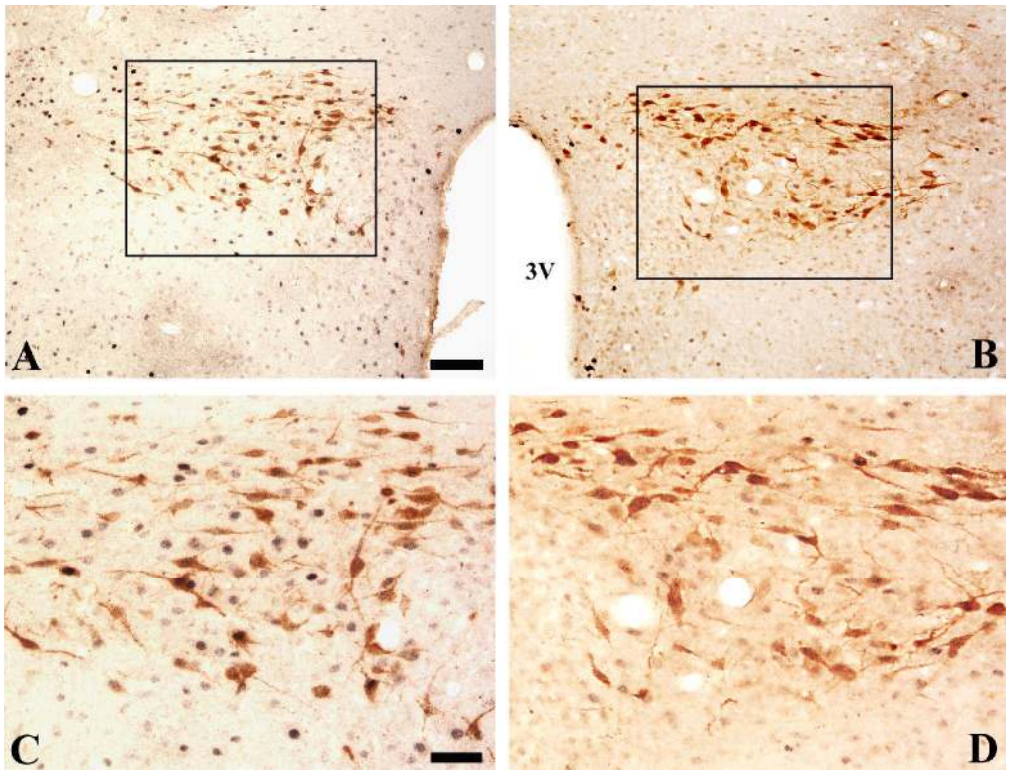

173x132mm (300 x 300 DPI)

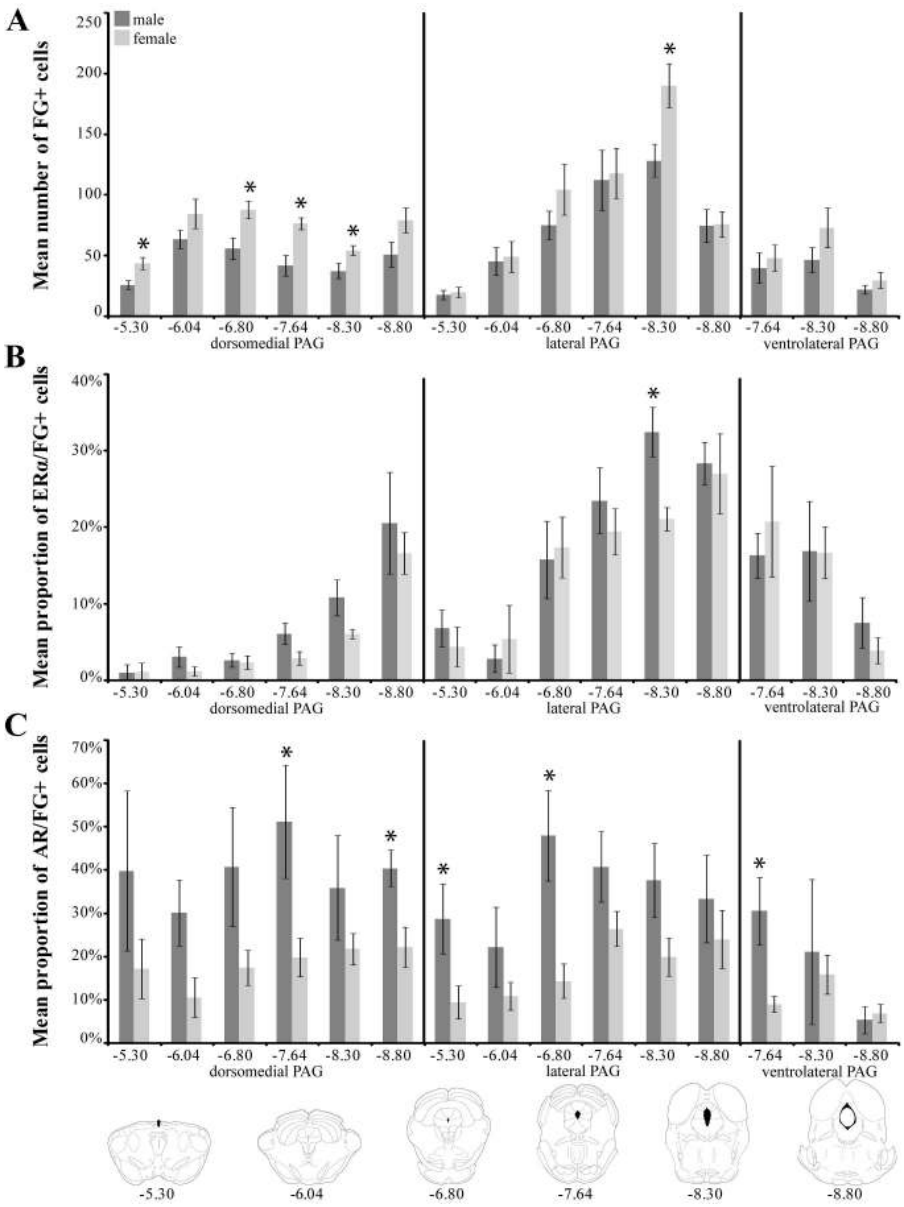

173x231mm (300 x 300 DPI)

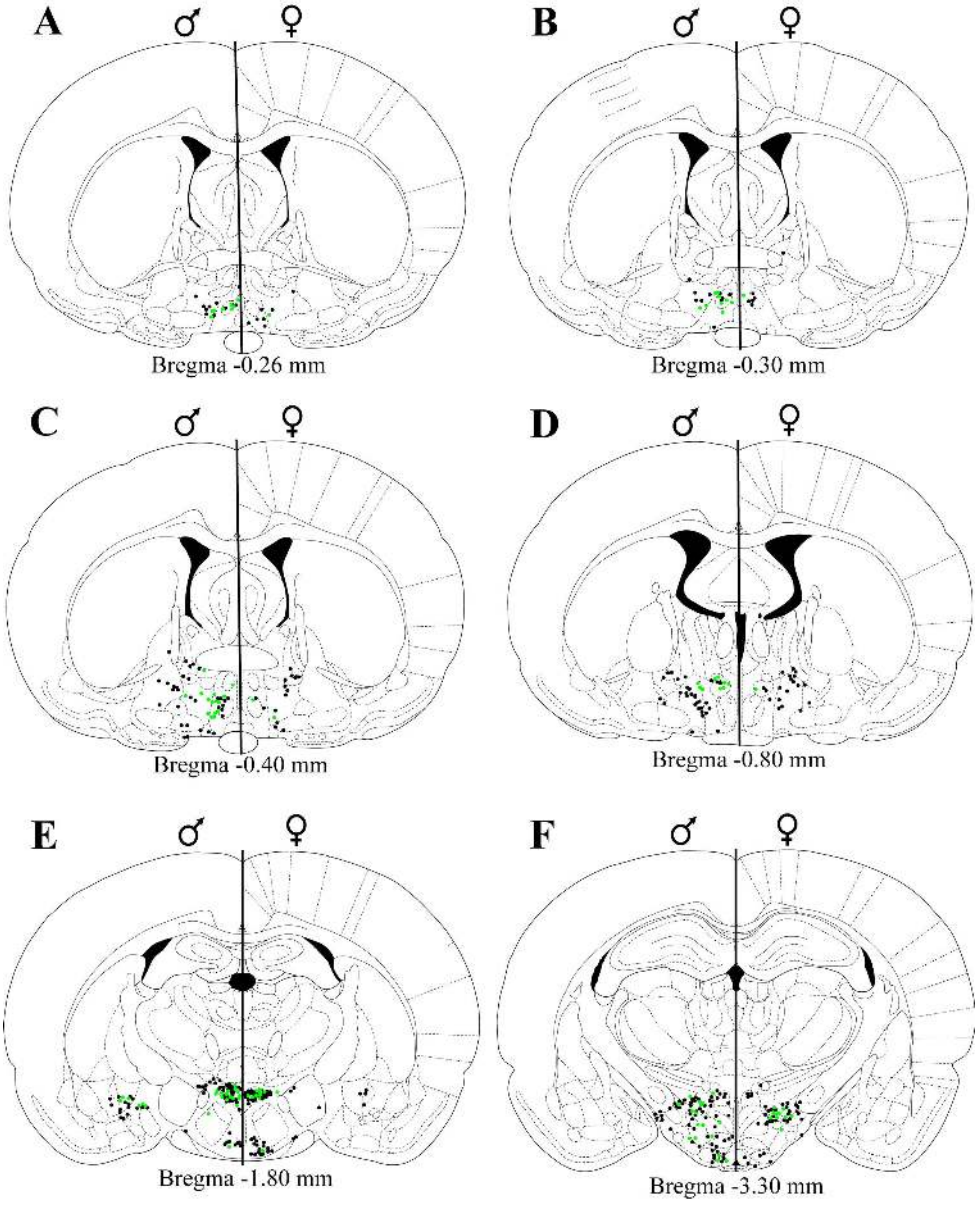

172x212mm (300 x 300 DPI)

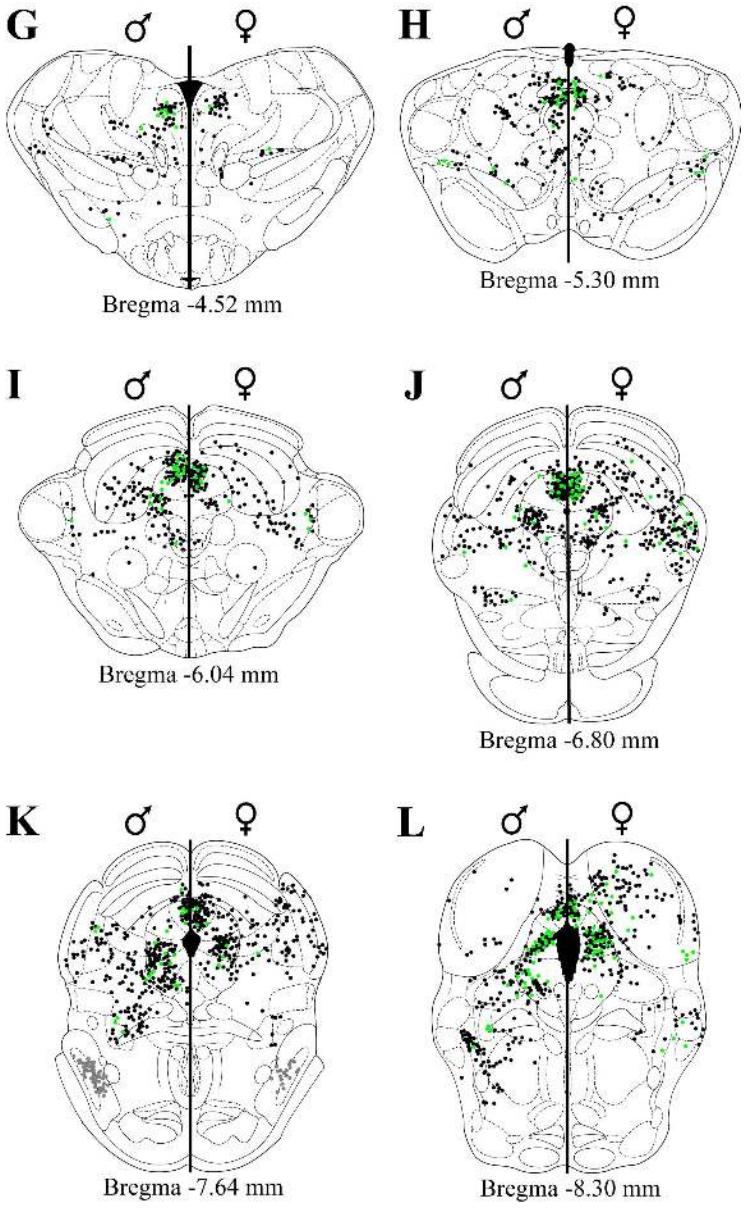

126x205mm (300 x 300 DPI)

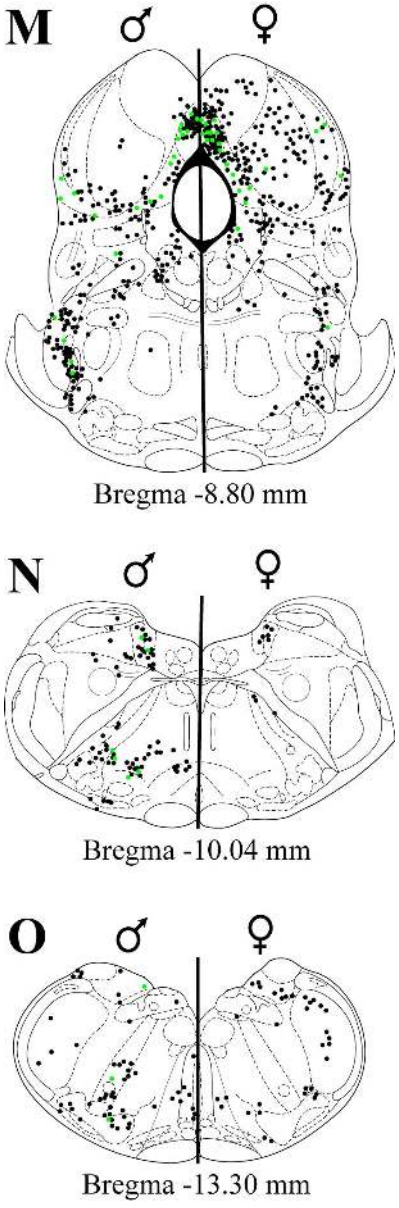

56x173mm (300 x 300 DPI)

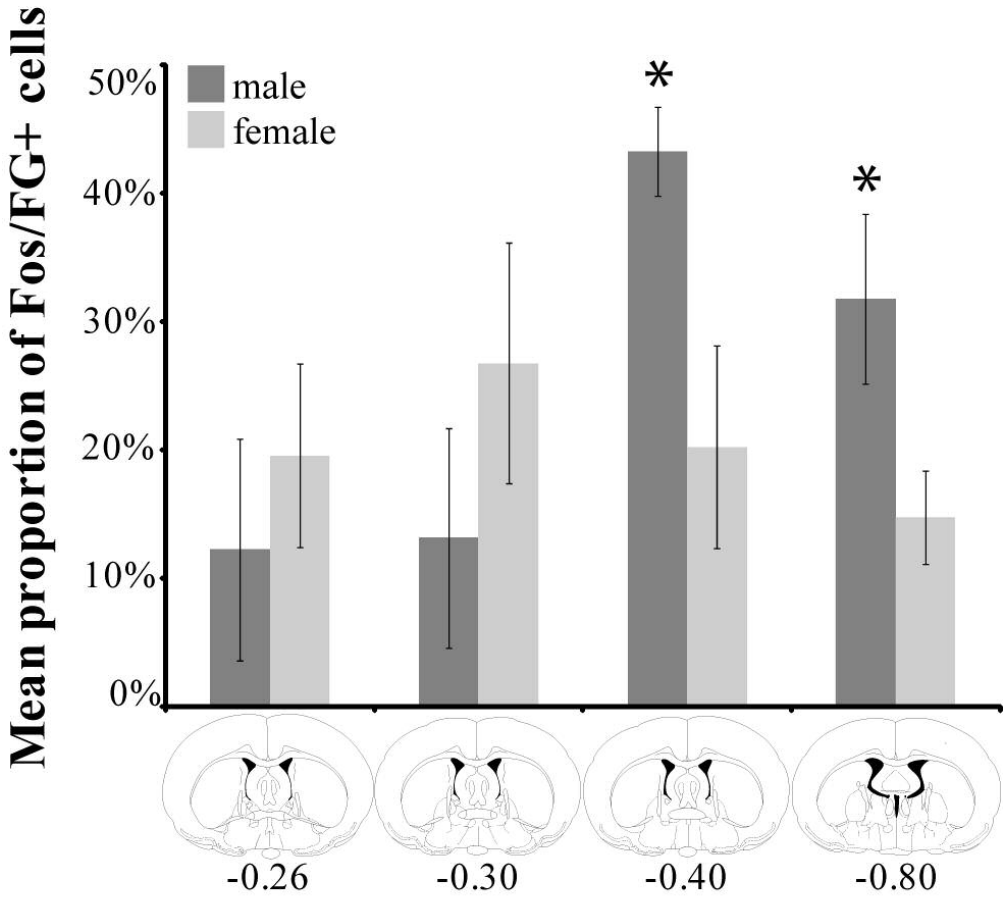

83x76mm (300 x 300 DPI)

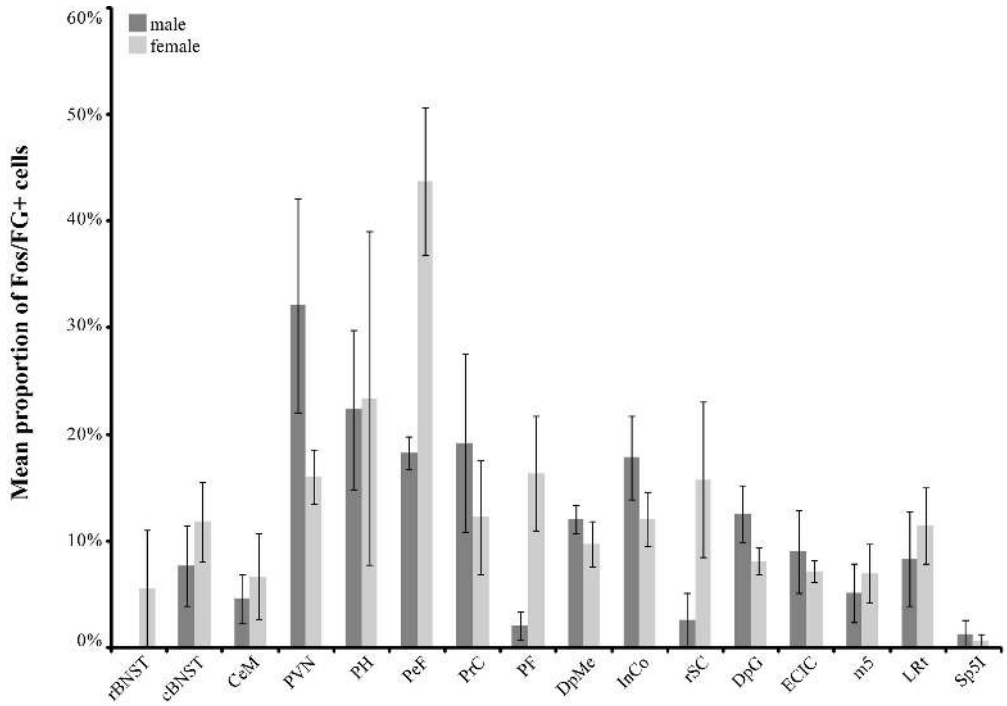

172x120mm (300 x 300 DPI)

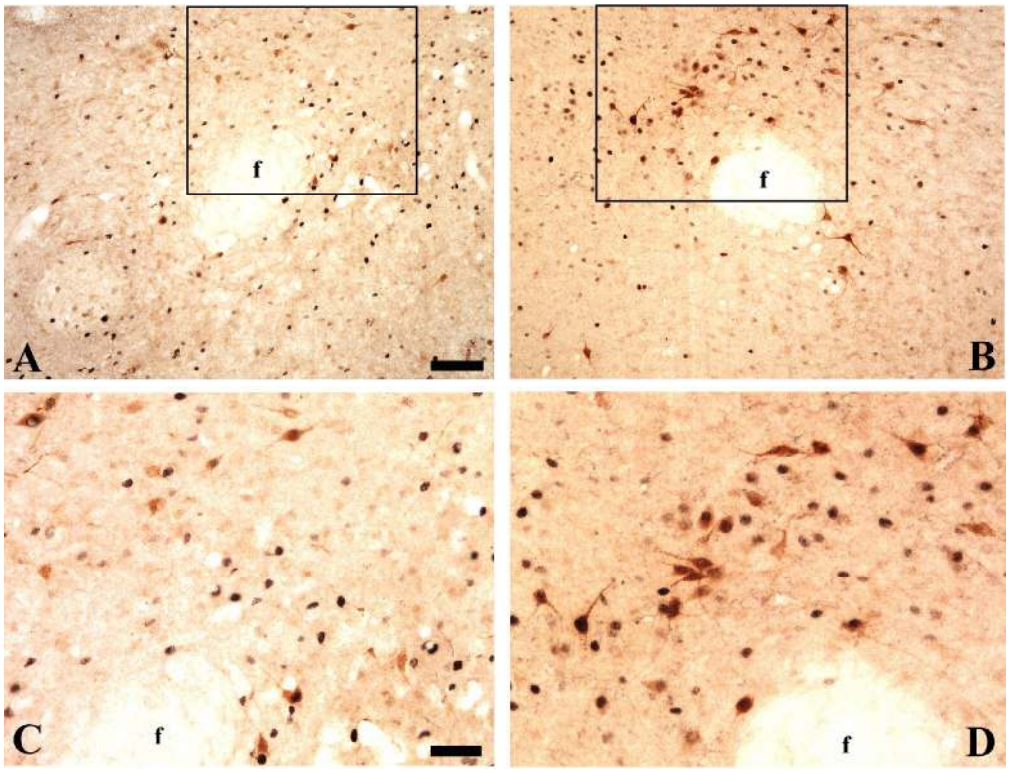

173x132mm (300 x 300 DPI)

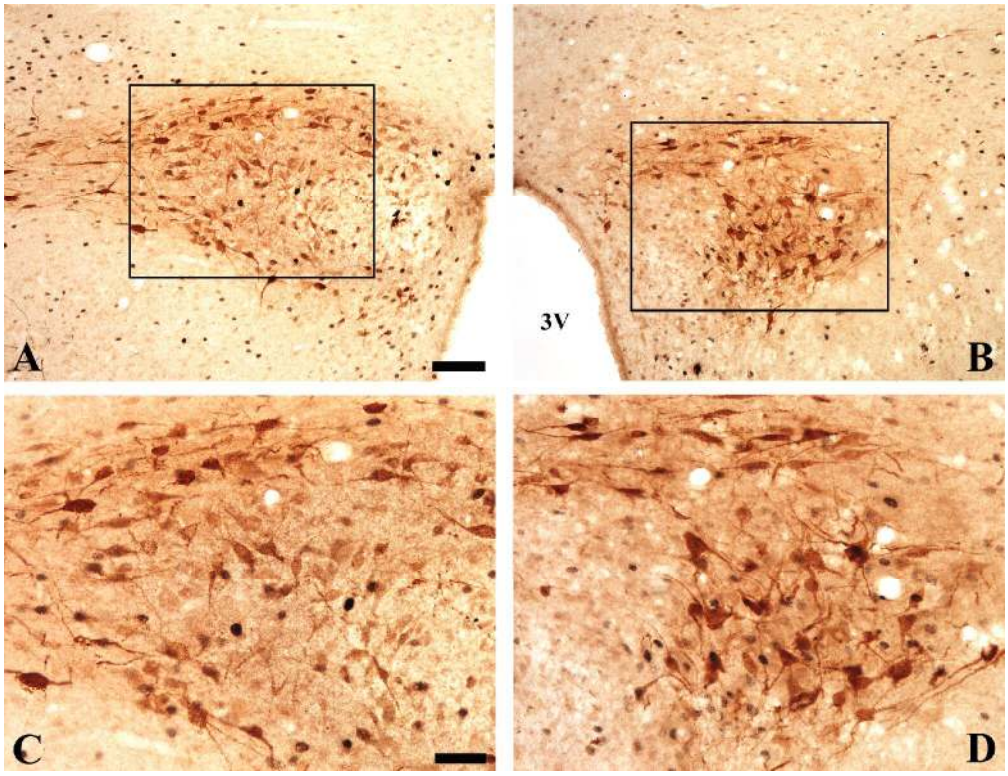

173x132mm (300 x 300 DPI)

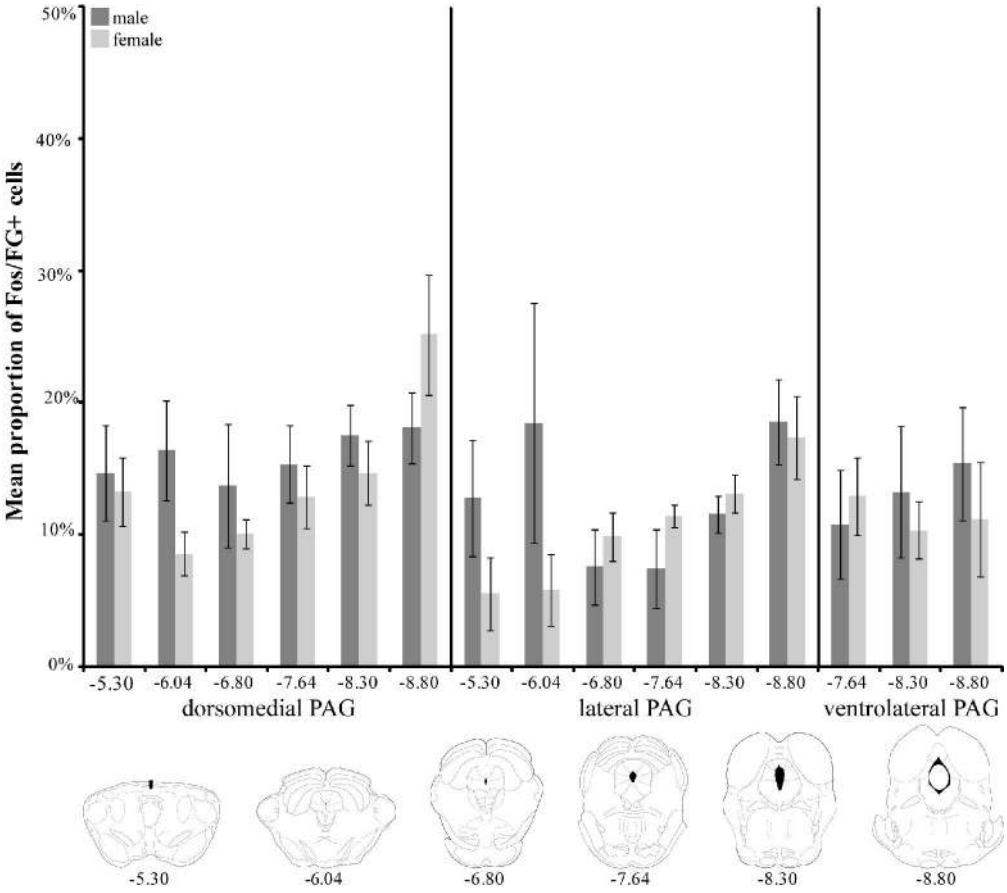

173x153mm (300 x 300 DPI)

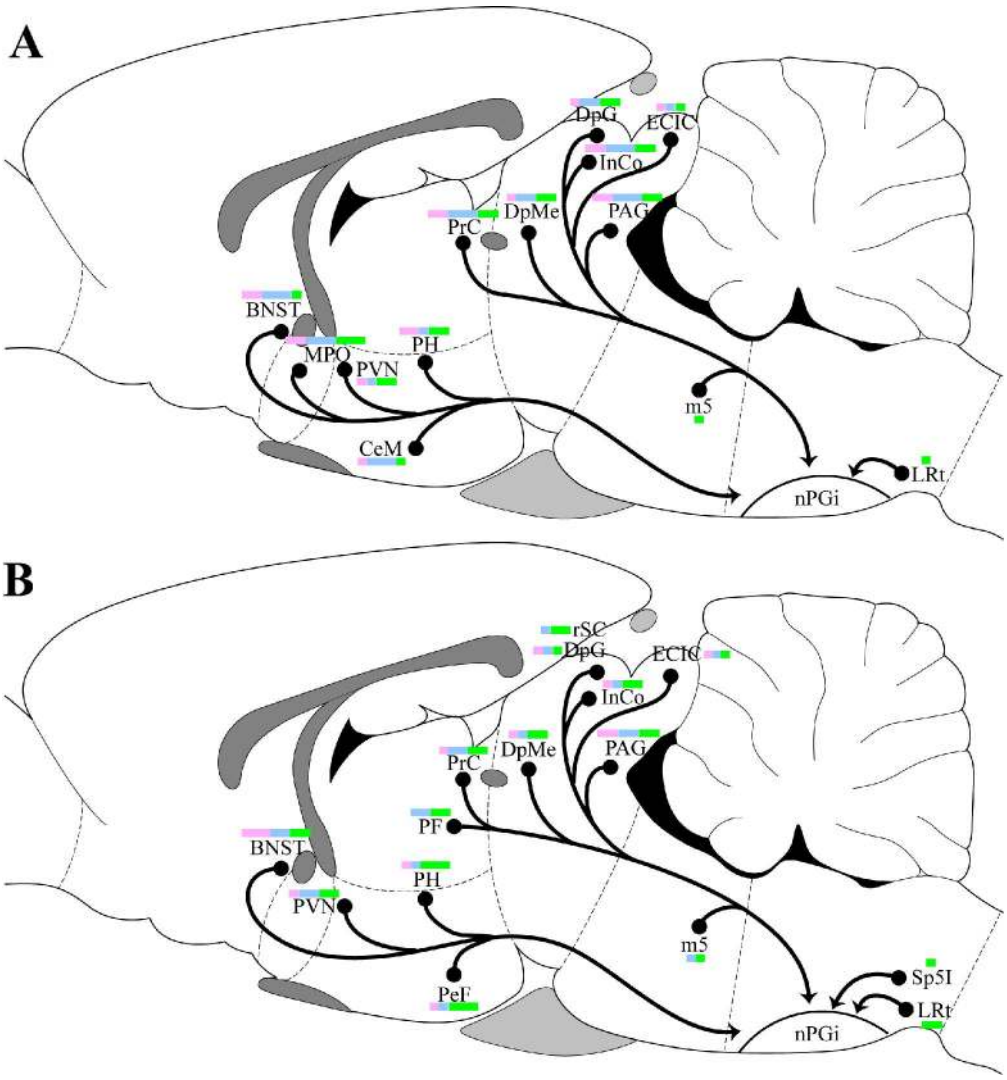

172x184mm (300 x 300 DPI)

Index of Abbreviations

3	oculomotor nucleus	PB	parabrachial nucleus
3V	third ventricle	PBP	parabrachial pigmented nucleus
4V	fourth ventricle	PCom	nucleus of the posterior commissure
AH	anterior hypothalamus	PCRt	parvicellular reticular nucleus
Arch	arcuate nucleus	PeF	perifornical nucleus
BIC	nucleus of the brachium of the inferior colliculus	PF	parafascicular thalamic nucleus
BNST	bed nucleus of the stria terminalis	PH	posterior hypothalamus
cBNST	caudal bed nucleus of the stria terminalis	PIL	posterior intralaminar thalamic nucleus
CeM	central amygdala	PL	paralemniscal nucleus
CnF	cuneiform nucleus	PLi	posterior limitans thalamic nucleus
Cu	cuneate nucleus	PnO	oral pontine reticular nucleus
dlPAG	dorsolateral periaqueductal gray	PP	peripeduncular nucleus
DM	dorsomedial hypothalamus	PPTg	pedunculopontine tegmental nucleus
dmPAG	dorsomedial periaqueductal gray	PR	prerubral field
DpG	deep gray layer of the superior colliculus	PrC	precommissural nucleus
DpMe	deep mesencephalic nucleus	PVN	paraventricular hypothalamus
dtg	dorsal tegmental bundle	py	pyramidal tract
ECIC	external cortex of the inferior colliculus	RCh	retrochiasmatic area
EW	Edinger-Westphal nucleus	RI	rostral interstitial nucleus of medial longitudinal fasciculus
f	fornix	RMC	magnocellular red nucleus
IMLF	interstitial nucleus of the medial longitudinal fasciculus	RPC	parvicellular red nucleus
InCo	intercollicular nucleus	RR	retrorubral nucleus
InG	intermediate gray layer of the superior colliculus	RRF	retrorubral field
IRt	intermediate reticular nucleus	rBNST	rostral bed nucleus of the stria terminalis
LC	locus coeruleus	rSC	rostral superior colliculus
LDTg	laterodorsal tegmental nucleus	SNCD	dorsal substantia nigra compacta
LH	lateral hypothalamus	SNL	lateral substantia nigra
lPAG	lateral periaqueductal gray	SNR	reticular substantia nigra
LPO	lateral preoptic area	Sol	nucleus of the solitary tract
LRt	lateral reticular nucleus	Sp5I	interpolar spinal trigeminal nucleus
m5	motor root of the trigeminal nerve	SPFPC	parvicellular subparafascicular thalamic nucleus
MCLH	magnocellular nucleus of the lateral hypothalamus	SubB	subbrachial nucleus
MCPC	magnocellular nucleus of the posterior commissure	SubI	subincertal nucleus
MeA	medial amygdala	TC	tuber cinereum area
Mo5	motor trigeminal nucleus	vlPAG	ventrolateral periaqueductal gray
MPO	medial preoptic area	VLTg	ventrolateral tegmental area
O	olivary nuclei	VMH	ventromedial hypothalamus
Op	optic nerve layer of the superior colliculus	VTA	ventral tegmental area
OT	nucleus of the optic tract	ZI	zona incerta

173x159mm (300 x 300 DPI)

Table 1 - Distribution of FG+ cells, and FG+ cells that also contained ERα, AR, or sex behavior-induced Fos following injection of FG into the nPGi.

			Male				Female			
	Region	Area	FG	ERα/FG	AR/FG	Fos/FG	FG	ERα/FG	AR/FG	Fos/FG
Diencephalon	*Preoptic Area*	MPO Rostral	+	++	+++	++	+	++	++	++
		MPO Caudal	++	+++	+++	+++	+	++	++	++
		LPO	+	++	+++	+	+	++	++	++
		BNST	+	+++	+++	+	+	+++	++	++
	Amygdala	MeA	+	++	++	++	+	+	++	+
		CeM	++	+	+++	+	+	++	+++	+
	Hypothalamus	PVN	++	+	+	++	+++	+	++	++
		AH	+	+	++	+	+	+	+	++
		LH	+	+	++	++	+	++	++	+++
		Rch	+	+	++	+	+	+++	+++	++
		PH	++	++	+	++	++	+	+	+++
		DM	+	-	++	++	+	++	+	+
		VMH	+	++	++	+	+	+++	+++	+++
		Arch	+	++	++	+++	+	++	+	++
		PeF	+	+	++	++	++	+	+	+++
		TC	+	++	+++	+	+	++	+++	+++
		MCLH	+	++	+++	+++	+	+	++	++
	Thalamus	PrC	++	++	+++	++	++	+	++	++
		PF	+	-	+++	+	++	-	++	++
		RI	+	-	+	-	+	-	+	++
		PR	+	-	+++	++	+	-	+	+
		SPFPC	+	-	-	+	+	-	-	+
		SubI	+	++	+++	++	+	+	+	++
		ZI	+	-	++	+	+	-	+	+
Mesencephalon	*Midbrain*	3	+	+	+	++	+	+	-	+
		EW	+	-	-	++	+	-	-	-
		PCom	+	-	+++	++	+	+	+	+
		MCPC	+	-	-	+	+	-	-	+
		IMLF	+	-	-	+	+	-	-	++
		DpMe	++	+	++	++	++	+	+	++
		RPC	+	-	-	++	+	-	-	-
		RMC	+	-	-	-	+	-	-	+
		RRF	+	-	++	++	+	-	+	+++
		PIL	+	-	-	+	+	-	++	+++
		PP	+	++	+	-	+	++	+	++
		SNL	+	+	++	++	+	-	+	+
		SNR	+	-	-	++	+	-	-	+
		PBP/SNCD	+	+	++	+	+	-	+	+
		InCo	++	++	+++	++	++	+	+	++
		OT	+	-	-	+++	+	-	+	+++
		PLi	+	-	+++	+++	+	-	-	+
		SubB	+	+	++	+	+	-	+	+
		VTA	+	-	-	+	+	+	-	-

173x212mm (300 x 300 DPI)

Table 1 (continued) - Distribution of FG+ cells, and FG+ cells that also contained ERα, AR, or sex behavior-induced Fos following injection of FG into the nPGi.

			Male				Female			
	Region	Area	FG	ERα/FG	AR/FG	Fos/FG	FG	ERα/FG	AR/FG	Fos/FG
Mesencephalon	*PAG*	dmPAG	+++	+	+++	++	+++	+	++	++
		dlPAG	+	-	+++	+	+	-	++	+
		lPAG	+++	+	+++	++	+++	++	++	++
		vlPAG	++	+	++	++	+++	++	++	++
	Superior Colliculus	rSC	+	-	+++	+	++	-	+	++
		Op	+	-	-	-	+	+	-	++
		InG	+	-	++	+	+	-	-	+
		DpG	++	+	++	++	+++	+	+	+
	Inferior Colliculus	BIC	+	+	+	+++	+	-	+	++
		ECIC	++	+	+	+	+++	+	+	+
Metencephalon	*Pons*	RR	+	-	-	-	+	-	-	-
		PPTg	+	+	++	++	+	-	-	+
		CnF	+	+	+	++	+	-	+	+
		dtg	+	-	+	+	+	-	-	-
		PB	+	-	+	+	+	-	+	+
		LDTg	+	-	+	+	+	-	-	+
		m5	++	-	-	+	+++	-	+	+
		PL	+	-	-	+	+	-	+	+
		PnO	+	-	-	+	+	-	-	+
		Mo5	+	-	+	-	+	-	-	+
		VLTg	+	-	+	-	+	-	-	-
		O	+	-	+	++	+	-	-	++
Myelencephalon	*Medulla*	LC	+	-	+	-	+	-	+	+
		Sol	+	-	+	-	+	-	+	-
		Cu	+	-	-	+	+	-	-	++
		GI	+	-	-	-	+	-	-	+
		IRt	+	-	-	-	+	-	-	-
		PCRt	+	-	+	+	+	-	-	-
		LRt	++	-	-	+	++	-	-	++
		Sp5I	+	-	-	+	++	-	-	+

173x155mm (300 x 300 DPI)

Table 2 - Sexual Behavior Measures (average) in Tracer-injected Male and Female Rats

Males			Females				
Mounts	Intromissions	Ejaculations	Mounts	Intromissions	Ejaculations	LQ	LR
14.2	43.8	4.8	24.7	33.7	3.7	0.99	1.95

173x20mm (300 x 300 DPI)